The Final Report

Title: New materials, techniques and device concepts for organic NLO chromophore-based electrooptic devices (Part 1)

Principal Investigator:

Marek Samoc, Ph.D., Professor
Laser Physics Center
Institute of Advanced Studies
The Research School of Physical Science and Engineering
Canberra ACT 0200
Australia
Telephone: +61-2-6125-4611
Facsimile: +61-2-6125-0029
E-mail: marek.samoc@anu.edu.au

Contract Number: FA5209-05-P-0131

AOARD Reference Number: AOARD-054010
(Continuation of this R & D is AOARD-054099)

AOARD Program Manager: Misoon Mah, Ph.D

Period of Performance: 29-Nov-04 – 29-Jan-06

Submission Date: 23-Aug-06

Report Documentation Page

Form Approved
OMB No. 0704-0188

1. REPORT DATE	2. REPORT TYPE	3. DATES COVERED
23 AUG 2006	**Final Report (Technical)**	**29-11-2004 to 29-01-2006**

4. TITLE AND SUBTITLE	5a. CONTRACT NUMBER
New materials, techniques and device concepts for organic NLO chromophore-based electrooptic devices (Part 1)	5b. GRANT NUMBER
	5c. PROGRAM ELEMENT NUMBER
6. AUTHOR(S) **Samoc Marek**	5d. PROJECT NUMBER
	5e. TASK NUMBER
	5f. WORK UNIT NUMBER
7. PERFORMING ORGANIZATION NAME(S) AND ADDRESS(ES) **The Australian National University,ACT,Canberra 0200,Australia,AU,0200**	8. PERFORMING ORGANIZATION REPORT NUMBER **AOARD-054010**
9. SPONSORING/MONITORING AGENCY NAME(S) AND ADDRESS(ES) **The US Resarch Labolatory, AOARD/AFOSR, Unit 45002, APO, AP, 96337-5002**	10. SPONSOR/MONITOR'S ACRONYM(S) **AOARD/AFOSR**
	11. SPONSOR/MONITOR'S REPORT NUMBER(S)

12. DISTRIBUTION/AVAILABILITY STATEMENT
Approved for public release; distribution unlimited

13. SUPPLEMENTARY NOTES

14. ABSTRACT
14. ABSTRACT DNA (deoxyribonucleic acid) has been characterized for photonic applications. The optical properties of DNA in various forms: both the native, sodium ion-based DNA, and a surfactant treated modification: DNA-CTMA were studied. The work covers study on interaction of DNA with dyes.

15. SUBJECT TERMS
Nonlinear Optical Materials

16. SECURITY CLASSIFICATION OF:			17. LIMITATION OF ABSTRACT	18. NUMBER OF PAGES	19a. NAME OF RESPONSIBLE PERSON
a. REPORT **unclassified**	b. ABSTRACT **unclassified**	c. THIS PAGE **unclassified**		**47**	

August 2006

Dr. Marek Samoc

Dr. Anna Samoc

Prof. Andrzej Miniewicz

Laser Physics Centre

Research School of Physical Sciences and Engineering

The Australian National University

Final Report for

Special Contract (AOARD-05-4010).

"New materials, techniques and device concepts for organic NLO chromophore-based electrooptic devices"

1. INTRODUCTION

This final report describes experiments carried out at Laser Physics Centre, the Australian National University as part of a research program on specially prepared materials based on DNA (deoxyribonucleic acid) for photonic applications. A part of the results obtained by us during this program has already been presented in our Interim Report. We present here some summaries and updates of these studies as well as numerous new results obtained after the Interim Report was submitted.

Our interest was in the optical properties of DNA in various forms: both the native, sodium ion-based DNA, and a surfactant treated modification: DNA-CTMA. We also present results referring to the interaction of DNA with dyes.

2. REFRACTIVE PROPERTIES OF DNA FILMS [1]

We report here a range of results on the refractive index in our DNA films, as well as the refractive index anisotropy and their dependence on film preparation and storage conditions. Using a prism coupler, we measured the refractive indices in

orthogonal directions: n_{TE}, light polarization direction parallel to the surface of the thin film, and n_{TM}, light polarization direction perpendicular to the surface of the thin film (i.e. inside the film depth). The DNA films were prepared from solutions of a high molecular weight DNA biopolymer (about 12 k base pairs). They were measured in ambient air with a relative humidity (RH) ranging from 37 to 58%. The refractive indices from prism coupler measurements were then used in the evaluation of the index dispersion, calculated from interference fringes in absorption and reflection spectra measured in the UV, visible and near infrared wavelength range.

2.1 EXPERIMENTAL

Material

Highly purified double-stranded sodium DNA was isolated from salmon milt and roe sacs (which are the waste products of the Japanese fishing industry) and purified by an enzymatic isolation process at the Chitose Institute of Science and Technology (CIST), as described in ref.[2] The average molecular weight of the received DNA was 8 x 10^6 Daltons (g/mol). This corresponds to 12 x 10^3 nucleotide base pairs (the average molecular mass of the nucleotide base pair, 662 g/mol, was counted without water molecules bound to the DNA).

DNA aqueous solutions of pH 6-6.5 were prepared at room temperature, 21-22ºC, by dissolving the fiber-like white solid material in deionized water. The concentration of DNA was in the range 0.1-3 wt %. The solutions were made using a typical procedure in which the components were placed in a glass vial; the vial was closed with PTFE-lined cap, and placed on a rotating wheel for about 24 hours for homogenization by solvent flow. Only the most concentrated solution (3 wt %) was homogenized with a magnetic stirring bar on a magnetic stage. The limit in the concentration, about 30 mg/mL of the high molecular weight salmon DNA, was due to the increasing viscosity of solutions. Lowering the molecular weight of the DNA, for example by ultrasonic processing, helps reduce the viscosity.[3] However, we did not utilize this treatment here because of the possible effect of scission on the structure and optical properties of the films.

It is known that the properties of the nucleate ions in solutions and films are dependent on the pH and ionic strength of the solution, the type of the counter-ions,

added electrolyte and the presence of other ions, temperature and even previous treatment of the nucleic acid. In this project we used aqueous, buffer-free, sodium ion-based DNA solutions of neutral pH, varying only the concentration of the solute and the method of film deposition. We characterized the solutions with electronic absorption spectra prior to the film deposition in order to learn about purity and the degree of denaturation of the solute, which was randomly selected from various batches of the supplied solid material. The spectra were measured with a UV-VIS-NIR spectrophotometer (Shimadzu, model 3101PC). They showed fair reproducibility of results and no sign of denaturation of the DNA. The average value of the specific absorption coefficient for the salmon DNA used, at the UV absorption maximum, λ_{max} = 258 nm, was found to be 18.1 ± 0.7 $(mg/mL)^{-1}$ cm^{-1}, corresponding to a molar absorption coefficient ε=(6.0 ± 0.2) x 10^3 $M^{-1}cm^{-1}$. This value is about 10 % lower than the literature data[4] for double-stranded DNA (from bacteria) in H_2O solutions at neutral pH, where ε = 6.6 x 10^3 M^{-1} cm^{-1} was measured for the absorption peak at 260 nm. This corresponds to a specific absorption coefficient equal to 20 $(mg/mL)^{-1}$ cm^{-1} = 0.020 $(\mu g/mL)^{-1}$ cm^{-1}. The lower ε value could be induced by a lower degree of purity of our material, different base composition or a hypochromic effect,[4-7] which gives a smaller ε for better orientated nucleotide bases in the double-stranded DNA. The absorbance ratio A_{260}/A_{280} is used as a relative spectroscopic measure of the nucleic acid purity with respect to the protein content in a sample. A typical A_{260}/A_{280} for pure, isolated DNA is 1.9.[7] A smaller ratio indicates increased contamination by proteins. The absorbance ratio A_{258}/A_{280}, which we evaluated in the measured spectra of solutions of randomly selected solid DNA fibers, gave an average value1.90 ± 0.02. These estimations are in agreement with the given percentage of purity of the salmon DNA used (96%), with a protein content of 2 %.[2]

Film preparation

Thin films of salmon DNA were prepared by casting and/or spinning of the DNA aqueous solutions on fused silica (Infrasil, GE I24) and ITO-coated glass substrates, 24 x 24 x 1 mm size. A Headway Research photo-resist spinner (model 1-EC101D-R485) was used for the film preparation. Films were dried in air, 21-22°C, RH about 40%, on a

laminar flow bench for about a day and stored in ambient air for several days. The list of films prepared out of the aqueous solutions of various Na-DNA concentrations is given in Table I. The various abbreviations of the films in Table I refer to the casting conditions only. A set of films (Table I) was additionally dried in a vacuum oven (Cole-Parmer) at a relatively low temperature range, 35-45ºC for 24 hours. The chosen temperature range should allow drying of the films without denaturation of the material and a hyperchromic effect. The time scale in Table I is calculated against the reference time zero when the set of films was removed from the vacuum oven (the sign "–" denotes the earlier time, which includes 24 hours of heating in the vacuum oven). The time between the film deposition and the end of the period of the vacuum drying was about 29 weeks for DNA-f1, about 6 days for DNA-f6, about 4 days for DNA-it6, about 5 days for DNA-f7, about 4 days for DNA-f8, and about 4 days for DNA-f9. After vacuum drying the films were stored in ambient air in a laboratory air-conditioned environment at a constant room temperature, 21-22ºC. However, relative humidity fluctuated a few percent within a day, and from day to day. In general, the films were exposed to the ambient air of RH level in the range 35% - 65%.

The relative humidity was measured with a weather station equipped with a mechanical hygrometer, a thermometer and a barometer. The RH data obtained with the analog hygrometer were comparable with the data measured with an electronic, digital thermo-hygrometer, Q-Trak Plus IAQ Monitor (TSI, Model 8554 with CO, the accuracy ±3% RH, resolution 0.1% RH).

The films absorption spectra were investigated in the wavelength range 200-3200nm using UV-VIS-NIR scanning spectrophotometers: Shimadzu (model UV-3101PC) and Varian Cary (model 5000). Prism coupler measurements enabling refractive index and film thickness determination were taken before and after the vacuum drying showing a response of a DNA film to a current humidity level. The response of refractive index of the films to the same RH level was reproducible within about 1 unit at the second decimal place. Thickness of the films was bigger in wet films, it decreased with drying and then increased at a higher humidity level. Thicknesses of films were measured with a prism coupler and also with a KLA-Tencor Instruments Alpha-step profiler (model 100). The thicknesses of prepared films ranged from 0.5 to 4.8 μm and for the various films were

not uniform through the entire sample area, but varied as it can be seen in Table I. The average thickness of the particular films was: 1.9 μm ± 0.4 μm in the film DNA-f1, 0.53 μm ± 0.04 μm in the film DNA-f6, 4.2 μm ± 0.5 μm in the film DNA-it6, 2.3 μm ± 0.3 μm in the film DNA-f7, 2.3 μm ± 0.5 μm in the film DNA-f8, 3.7 μm ± 0.7 μm in the film DNA-f9. The standard deviation indicates the magnitude of the variation of a film thickness at the spots measured in various regions of a film.

Prism coupler measurements

Refractive indices of the films were determined with the prism coupling technique utilizing optical waveguiding in a film.[8, 9] The indices were measured with a Metricon Prism Coupler, model 2010 (www.metricon.com), using a procedure in which the film is being brought into contact with the base of a prism by means of a pneumatically-operated coupling head. A laser beam, about 1-2 mm in diameter, with a wavelength of either 632.8 nm or 814 nm, is directed through the prism, striking the base of the prism at the coupling spot. The light beam is normally totally reflected at the prism base, and is collected by a photodetector. However, at certain values of the incidence angle, light can tunnel across the air gap between the film and the prism at the coupling spot, and enter into a waveguiding optical propagation mode in the film. This induces a sharp drop in the intensity of light reflected from the base of the prism and creates a dip in the reflectance curve measured by the detector. See Fig. 1. The index of the film is derived from the light propagation constant determined by the angular location of the modes and the index of the prism. The prism coupler measures the index of refraction of the film at the laser wavelength and can provide the film thickness, if the film is sufficiently thick to support two or more optically guided modes. The instrument specification for the accuracy and resolution is ± 0.001 for index accuracy and ± 0.0005 for index resolution. The thickness accuracy is ± 0.5 % and the thickness resolution is ± 0.3 %.

Figure 1 shows examples of the reflectance curves obtained with the Metricon prism coupler in a DNA film using the transverse electric (TE) plane polarized light and the transverse magnetic (TM) plane polarized light. For TE polarization the electric field vector is parallel to the substrate, for TM polarization the magnetic field vector is parallel to the substrate.

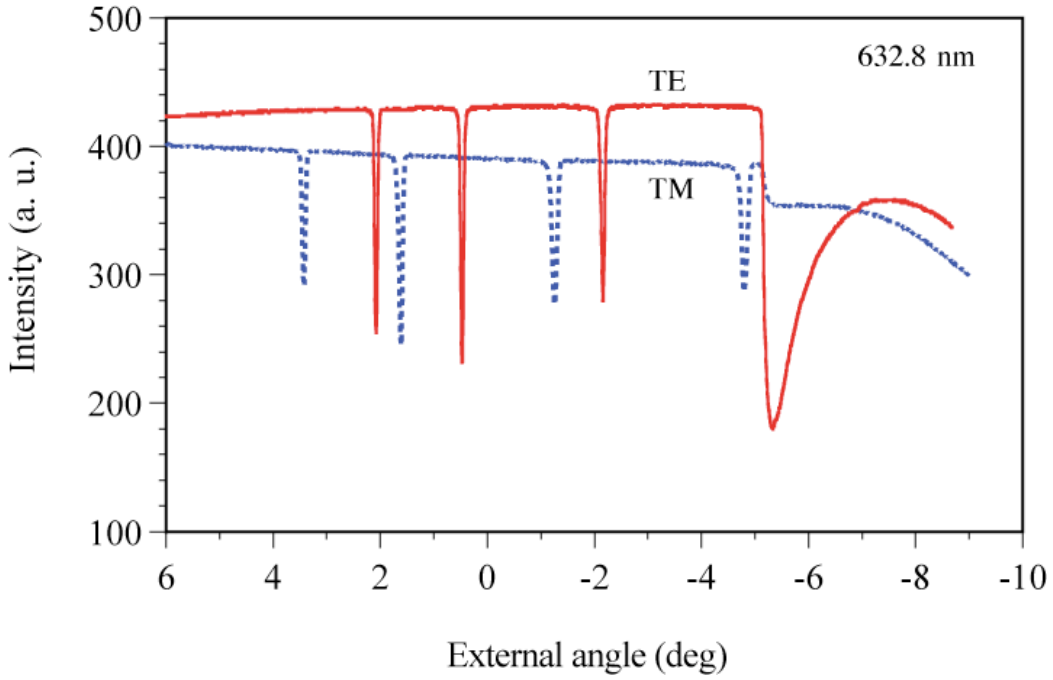

Figure 1. Prism coupler reflectance curves measured in a film of salmon DNA (DNA-f7) on a silica substrate at an RH ~50%. The refractive indices: n_{TE} = 1.5445, n_{TM} = 1.5597 at λ = 632.8 nm, and the thickness 2.05 μm were computed from the modes obtained for TE and TM polarization of He-Ne laser light in the film. The film was dried in vacuum at 35-45°C for 24 hours then stored for 1 day in air prior to the prism coupler measurements.

2.2.RESULTS AND DISCUSSION

Anisotropy of refractive index

Refractive indices *n* for the orthogonal TE and TM light polarizations are reported for six DNA films in the Table I. The refractive index data are presented against time, since the film was dried under vacuum at a slightly elevated temperature (35-45°C).

TABLE I

Refractive indices *n* of DNA films measured with a prism coupler in ambient air, 22°C

Film, substrate, method, solution conc.	Time since drying (week)	RH (%)	n_{TE} 632.8nm	n_{TM} 632.8nm	n_{TE}-n_{TM} 632.8nm	Thickness (μm)
DNAf1,	0.04	45	1.5577	1.5563	0.0014	2.1
Infrasil,	9.7	39	1.5480	1.5402	0.0078	1.5
cast & spin, 600 rpm,	12.0	55	1.5371	1.5320	0.0051	1.7
3 wt %	13.6	53	1.5293	1.5357	- 0.0064	2.4
DNAf6,		40	1.5367	1.5627	- 0.0260	0.50
Infrasil,	0.04	45	1.5483	1.5671	- 0.0188	0.59
spin, 200-700 rpm,	9.7	38	1.5338	1.5330	0.0008	0.50
many layers,	12.6	58	1.5184	1.5454	- 0.0270	0.53
0.15 wt %	13.6	53	1.5309	1.5675	- 0.0366	0.53
DNAit6		40	1.5352	1.5612	- 0.0260	3.9
ITO/glass,	0.04	45	1.5468	1.5633	- 0.0165	4.0
spin, 120 rpm	2.9	55	1.5263	1.5369	- 0.0106	4.7
many layers,	12.2	53	1.5130	1.5349	- 0.0219	4.0
0.15 wt %	13.6	53	1.5145	1.5409	- 0.0264	4.6
DNAf7		41	1.5362	1.5607	- 0.0245	2.1
Infrasil		39	1.5363	1.5608	- 0.0245	2.2
cast,	0.02	45	1.5486	1.5654	- 0.0168	2.1
0.20 wt %	0.17	50	1.5446	1.5597	- 0.0151	2.0
	3.0	50	1.5234	1.5420	- 0.0186	2.5
	9.6	37	1.5424	1.5448	- 0.0024	2.0
	12.2	53	1.5212	1.5403	- 0.0191	2.6
	12.6	58	1.5153	1.5403	- 0.0250	2.4
	13.6	54	1.5126	1.5417	- 0.0291	2.7
DNAf8,		37	1.5361	1.5668	- 0.0307	2.2
Infrasil,		38	1.5367	1.5662	- 0.0295	2.2
cast,	0.02	45	1.5474	1.5732	- 0.0258	1.8

0.11 wt %	3.0	50	1.5225	1.5544	- 0.0319	2.4
	9.7	45	1.5339	1.5628	- 0.0289	1.8
	9.7	42	1.5353	1.5639	- 0.0286	1.8
	9.7	40	1.5365	1.5648	- 0.0283	1.8
	12.2	54	1.5062	1.5360	- 0.0298	3.0
	12.6	56	1.5126	1.5431	- 0.0305	3.0
	13.6	53	1.5137	1.5442	- 0.0305	2.9
DNAf9		39	1.5362	1.5616	- 0.0254	4.8
Infrasil,		40	1.5361	1.5622	- 0.0261	4.4
spin,	0.02	45	1.5505	1.5664	- 0.0159	3.9
120-300 rpm	3.0	50	1.5366	1.5420	- 0.0054	3.8
0.19 wt %	9.7	38	1.5418	1.5469	- 0.0051	3.2
	9.7	38	1.5426	1.5458	- 0.0032	3.8
	12.2	53	1.5309	1.5366	- 0.0057	3.1
	12.6	56	1.5282	1.5407	- 0.0125	3.3
	13.6	54	1.5204	1.5462	- 0.0258	2.5

Films were dried in vacuum at 35-45°C for 24 hours then stored in air

We were concerned about the identity of the material and uniformity of the films at various coupling spots. We checked the reproducibility of the values of refractive indices measured with light coupled into different spots on films. The index values did not change substantially. For example, the difference between the n values measured at two spots was only 1 x 10^{-4}, both for n_{TE} and n_{TM}, in the film DNA-f7, (1-7) x 10^{-4} in the film DNA-f8, and (1-5) x 10^{-4} in the film DNA-f9, before vacuum drying. The n values were found to be different at two different places by about 9 x 10^{-4} on the film DNA-f9 when the film was measured at an RH of 38% after 10 weeks after drying. Therefore, we conclude that optical properties did not vary substantially from spot to spot in these films. Also, the index fluctuation was within the instrument specification on the index accuracy measurements. However, the thickness of films varied markedly between samples, from spot to spot. The change ranged from a few percent in thinner films to about 20 percent in thicker films.

We observed that the refractive indices of DNA films were highly sensitive to the drying conditions and humidity of the environment during measurements and storage (this effect is suppressed in DNA-CTMA films, as reported in detail elsewhere). Figure 2 shows the refractive index data (plotted from Table I) which we measured in DNA films in ambient air of different relative humidity. The indices dropped markedly when the humidity in the laboratory environment reached a level of 55-60%.

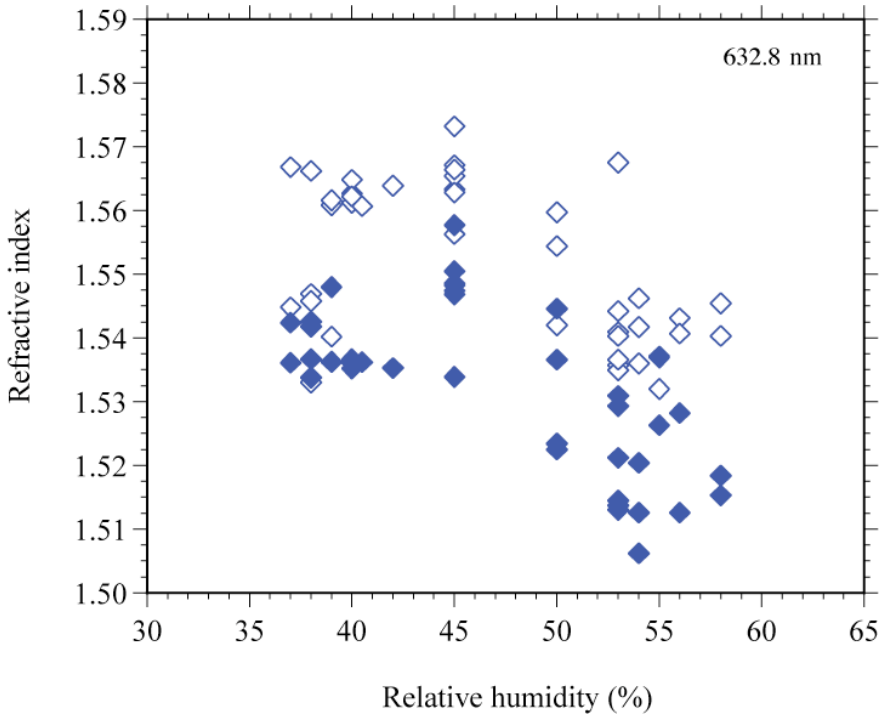

Figure 2. Refractive indices n_{TE} (filled diamonds) and n_{TM} (open diamonds) for six DNA films measured with a Metricon prism coupler at λ = 632.8 nm, 22°C, before and after vacuum drying for 24 hours at 35-45°C, and during 3 months of storage in ambient air of different relative humidity.

An interesting observation can be made regarding birefringence of the films. In most of the DNA films the n_{TE} values (electric field vector parallel to the surface of the film) were lower than the n_{TM} (electric field vector perpendicular to the surface of the film or along the film thickness). The birefringence, $\Delta n = n_{TE} - n_{TM}$, was as high as -0.032 in some films. Such a high value of the negative birefringence suggests a high degree of the

orientation of DNA molecules in a film. This can be deduced on the basis that the polarizability of the rigid-rod DNA molecule is larger in the direction perpendicular to the double helix axis than along it, due to a parallel stacking of the highly polarizable, anisotropic aromatic nucleotide bases. Therefore, the refractive index in the direction parallel to the nucleotide bases (i.e. across the DNA helix) is larger than along the length of the molecule axis. The higher value of refractive index observed for the E-field polarization direction perpendicular to the surface of the film suggests that the rigid-rod DNA molecules lay mostly parallel to the surface of the film.

The chain alignment in DNA films was induced spontaneously during film preparation, in the process of drying the diluted solutions. Evaporation of the solvent causes formation of a concentrated layer near the surface, the molecules can align along the air-liquid interface at the surface due to the "interfacial effect".[10] In this mechanism an evolution of a concentrated layer near the surface may lead to the transitional formation of a nematic-like liquid crystalline phase, resulting in an anisotropic birefringent DNA film with good polymer chain alignment and orientation.

A careful inspection of the results in Table I reveals that some of our films were highly anisotropic, molecules were aligned parallel to the film surface, some were nearly isotropic and some even had an opposite anisotropy. The different structures of the films arise as a result of the different preparation and environmental storage conditions. Fig. 3 shows refractive indices for TE and TM polarization in two selected films (data from Table I). The film DNA-f1, prepared by spinning of a more concentrated solution (3 wt % DNA), was almost isotropic, where film DNA-f7, prepared by casting from a diluted DNA solution (0.20 wt % DNA) on an identical substrate, was highly birefringent. The refractive properties of these films were also influenced by the humidity, however, in a different way.

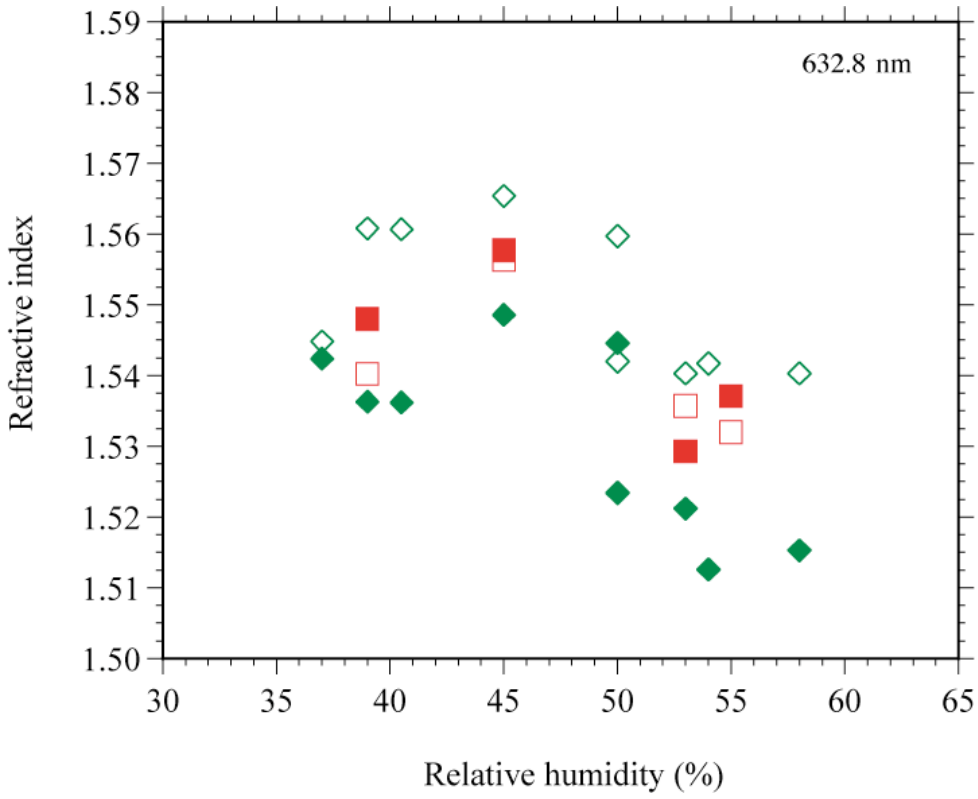

Figure 3. Refractive indices at $\lambda = 632.8$ nm of two selected DNA films measured with a prism coupler at 22 ºC in air of different relative humidity, before and after vacuum drying (35-45ºC, 24 h). Filled squares are for n_{TE}, open squares are for n_{TM} in spin-coated film DNA-f1 prepared from 3 wt % DNA aqueous solution. Filled diamonds are for n_{TE}, open diamonds are for n_{TM} in the film DNA-f7 prepared by casting of 0.20 wt % DNA aqueous solution, also on Infrasil substrate.

A small positive birefringence ($n_{TE} > n_{TM}$) in a spin-deposited film of DNA-f1 (data represented by squares in Fig. 3) indicated that the orientation of the DNA molecules was almost isotropic with some orientation in the direction perpendicular to the surface of the film (the molecules adopted a spherulitic-like form). This weak birefringence changed sign at an RH of 53%.

The other strongly negatively birefringent film, DNA-f7, had molecules highly aligned in the plane parallel to the surface ($n_{TM} > n_{TE}$). Refractive indices were larger at a lower humidity, but the birefringence almost disappeared at an RH of 37 %. The same happened to the spin-deposited film DNA-f9. The spin-deposited film of DNA-f6

showed an inversion in the sign of the birefringence at an RH of about 38%. These observations could be explained by polymorphism of DNA and by the phase transitions observed in crystalline and semicrystalline fibers and films upon swelling and dehydration.[6, 11, 12]

It is possible that the mechanism of alignment of DNA chains may involve the formation of mesoscopic nematic, smectic and cholesteric liquid crystalline phases when the solvent evaporates during film formation, when the solute concentration reaches a critical value. Kagemoto et al.[13] showed that the phase states of DNA in concentrated solutions changed from an isotropic phase at DNA concentration below 2 wt %, to an anisotropic phase in the concentration range of 3-5 wt % DNA, and to a liquid crystalline phase at concentrations above 6 wt % DNA. The formation of lyotropic liquid crystalline phases in more concentrated DNA solutions in the range of 100-300 mg/mL was also studied, for example, by Brandes and Kearns,[14] Strzelecka,[15, 16] Van Winkle,[17, 18] Rill,[19] Leforestier.[20] Supramolecular hexagonal columnar organization[21] and the formation of a hexatic phase between the cholesteric and the crystalline phases have been reported for oriented DNA sheets.[22] The formation of ordered structures in films following drying of 30-60 mg/mL solutions was reported in papers by Morii.[10]

We inspected the morphology of DNA films with cross-polarized white-light microscopy under low magnification. Preliminary observations revealed the presence of textures and patterns of stripes, distinctly ordered at the films thicker edges, and occasionally, colors, which might be related to the presence of the liquid crystalline phases in the films.

Our DNA films showed a higher degree of birefringence and a better chain alignment than that reported for films of the higher molecular weight, 29 k base pairs, salmon DNA, where the highest (negative) birefringence was 0.027.[10] Brandes[14] observed a birefringence of 0.02 ± 0.005 in a magnetically ordered liquid crystal at a concentration of 248 mg/ml calf thymus DNA. The difference in liquid crystalline behavior and optical properties can be accounted for by a different molecular weight of DNA, concentration of the solute, the presence of electrolyte ions, and a speed of film drying.

We see from our data that it is possible to obtain molecularly-oriented DNA films with an isotropic or anisotropic chain orientation which is orthogonal to the planar

orientation, found in most of our films. A strong positive birefringence in the DNA film, reported by Wang[23] and Zhang,[24] where $n_{TE} = 1.534$ and $n_{TM} = 1.497$, might have origin in a film structure generated by the method of film processing and material preparation conditions, however, these parameters were not specified.

The values and the anisotropy of the refractive indices found in our solution cast films, are in a good correspondence with the data obtained by Rupprecht and coworkers[25] in a stretch-oriented, about 50 μm thick fibril-like, films of Na-DNA. The indices, measured at $\lambda = 514.5$ nm, responded to the relative humidity and were anisotropic. The refractive index perpendicular to the drawing axis was 1.551 ± 0.009 at an RH of 45 %. It was larger than the index in the direction parallel to the drawing axis, 1.505 ± 0.005 at an RH of 45%.[25] These films were negatively birefringent, the Δn was about 0.04 - 0.05 throughout most of the humidity range, and they were highly crystalline. The indices decreased with increasing water content, like in our films. An anomalous behavior was observed at an RH of between 70 and 86 %,[11, 26] that was accounted for by the transition from the A to B phase of DNA (the B phase occurs at a higher water content).

The optical constants of a DNA film in vacuum were measured by Inagaki,[27] $n = 1.58$ at $\lambda = 620$ nm and $n = 1.59$ at 496 nm. Presumably, they were obtained in the film plane. They coincide poorly with the value 1.552 ± 0.007 measured at $\lambda = 514.5$ nm in vacuum, in the stretch-oriented film, in the direction parallel to the drawing axis in ref.[26] Surprisingly, they are similar to the n data for the film in a vacuum, in the direction perpendicular to the drawing axis, 1.583 ± 0.006.[26]

These observations indicate that DNA is an exceptionally complex material, which requires rigorous handling procedures and well-defined conditions of the film preparation methods in order to be able to predict film properties. Of special interest, as a possible tool to control the orientation and anisotropy of DNA films, are unique methods of preparation of oriented lyotropic liquid crystalline films successfully developed by Kryszewski's group.[28-30]

Dispersion of the refractive index

Inagaki[27] measured the wavelength dependence of n in a DNA film in a vacuum as well as at an RH of 92 % in the range 2 – 4 eV (λ = 620 – 310 nm). The change in the relative humidity dramatically reduced the n value from 1.58 at an RH of 0 % to about 1.43 at an RH of 92 %, at a photon energy of 2 eV.

The electronic spectra of DNA films show a prominent absorption peak at λ = 260 nm, a valley at λ = 231 nm in the UV range, and a relatively strong absorption peak in the IR range. This peak, with a maximum at about λ = 2990 nm and a side band at about λ = 3120 nm, is caused by oscillation vibrations of the O-H and N-H bonds. The height of this peak depended on the relative humidity and the content of water in DNA films.

Absorption and reflection spectra of thin DNA films can often display fringes due to the interference of light being transmitted through the film, with that reflected from the other interface. Fig. 4 shows an example of fringes in the absorption spectrum measured in a 2.07 μm thick film of DNA-f7 on a silica substrate.

We derived the dispersion of n in our DNA films from the interference fringes measured in the absorption and reflection spectra in a wide spectral range, λ = 200 to 3200 nm, at normal and oblique angles of incidence, respectively, employing a Cary 5000 and a Shimadzu spectrophotometer. It provided data for a comparison to the results obtained using the prism coupling technique.

Transmission of light through a thin film depends on the values of the refractive index of the film $n(\lambda)$ and of both the substrate and the upper dielectric medium (air). A transmission spectrum contains fringes whose positions can be approximated from the relation $I(\lambda) = I_0 \sin(2k(\lambda)d + \Delta\phi)$, where $k(\lambda) = 2\pi n(\lambda)/\lambda$ is the light propagation vector in the medium and $\Delta\phi$ is a phase shift. The positions of these fringes can be used to obtain information on the thickness and the refractive index of the film, e.g. by the method of Swanepoel.[31] For light with normal incidence on a film of thickness d, the wavelengths of the transmission extrema are given by the well-known relation: $2nd = m\lambda$, where m is the integer number counting maxima. In practice, $n(\lambda)$ can be estimated for transparent films of thickness ranging from 0.5 μm to 5 μm.

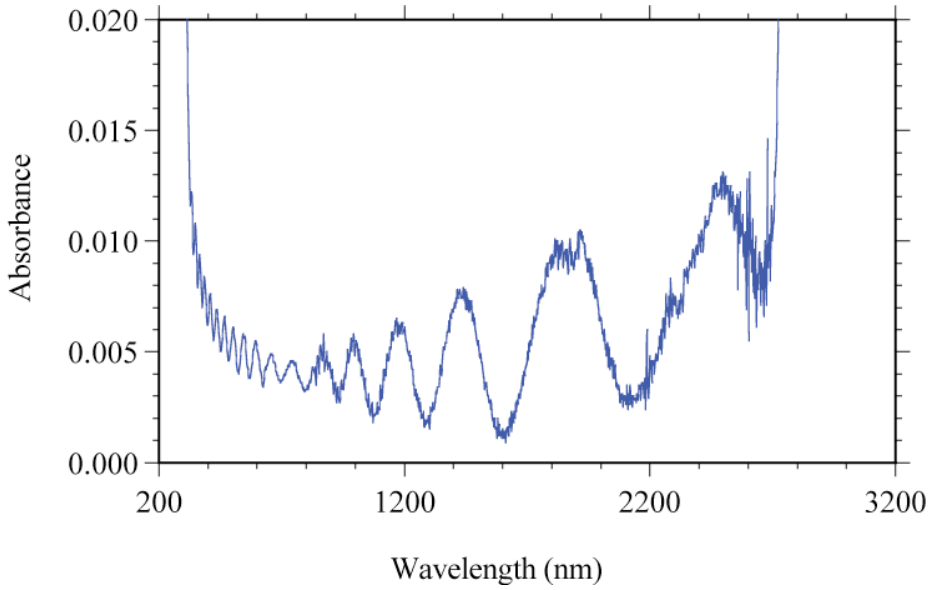

Figure 4 The interference fringes in absorption spectrum of DNA-f7 film on Infrasil substrate measured in air, RH ~ 45%, immediately after drying in vacuum (35-45°C for 24 h). The thickness of the film, 2.07 μm, derived from fitting of the fringe pattern, using n_{TE} = 1.5486 at λ = 632.8 nm, and 1.5406 at λ = 814 nm, is in fair agreement with thickness of the film, 2.09 μm, measured with the prism coupler.

We analyzed the interference fringes in the absorption spectra in order to derive the thickness of the films, the refractive index n and its dispersion. We used a method similar to that of Swanepoel in the approach, in which we made use of the knowledge of the refractive index of the film at a single wavelength and applied the Sellmeier dispersion equations for fitting of the transmission fringes in a broad wavelength range. We have chosen to approximate the index dispersion $n(\lambda)$ by a Sellmeier-type formula

$$n(\lambda) = \left(A + \frac{B}{1 - \frac{C}{\lambda^2}} \right)^{0.5}, \qquad (1)$$

which requires knowledge of the dispersion parameters A, B and C.

We performed many measurements of absorption and reflectance spectra of pure DNA films listed in Table I. The fringe patterns were fitted using the Mathcad 2000 program, adjusting parameters in the Sellmeier formula to achieve the same number and position of all the measured maxima and minima in the entire spectral region.

The refractive indices of DNA depended on a marked degree on factors, such as the relative humidity, as shown in Table I. From the measurements, an 'average' index dispersion formula was derived, i.e. a Sellmeier type equation, which can be used in the case of our DNA films. For salmon DNA films prepared from deionised water solutions we have found a relation:

$$n(\lambda) = \left(1.028 + \frac{1.286}{1 - \frac{14000}{\lambda^2}} \right)^{0.5}, \qquad (2)$$

where λ is in nm. In the case of DNA films for which the refractive index is very sensitive to the content of water, the first parameter (A) of the equation had to be varied to some extent in order to obtain a good fit to the measured thickness and refractive index for films under different humidity conditions, while the B and C parameters did not require such variation. Equation (2) gives $n_{TE} = 1.5364$ at $\lambda = 632.8$ nm, $n_{TE} = 1.5303$ at $\lambda = 814$ nm, as possible values of refractive index, for example at an RH ~ 50 %.

The fitting of the fringes in the spectrum in Figure 4, for DNA film DNA-f7, 2.07 μm thick, measured at an RH ~ 45%, gave the dispersion parameters $A = 1.0655$, $B = 1.2858$, $C = 14000$. Absence of “in plane” anisotropy has been detected for the refractive index of studied DNA films, at least within the accuracy of absorption and reflectance methods. The prism coupler values, $n_{TE} = 1.5486$ at $\lambda = 632.8$ nm and 1.5406 at $\lambda = 814$ nm, were obtained in this film at an RH ~ 45%, following the measurement of the spectrum in the same film area. For the measurements of reflection spectra we used a Variable Angle Specular Reflectance accessory (VASRA) designed for the Cary 5000 spectrophotometer, allowing for reflectance measurements at angles between 20 and 70 degrees. However,

we will report this in detail elsewhere. The use of the absorption interference fringes technique can be advantageous for the studies of uniformity of the optical properties of DNA-based films.

2.3 CONCLUSIONS

Our films of double-stranded DNA, derived from salmon milt and roe sacs, have demonstrated interesting linear optical properties. We prepared a series of films using both spin-coated and cast aqueous solutions, in a range of concentrations of DNA solute, 0.1-3 wt %. The solutions were characterized with absorption spectra. Films were measured with a prism coupling technique to obtained refractive indices for TE and TM light polarization. The absorption and reflection spectra showed interference fringes, which could be used to derive information on refractive index dispersion.

We observed that the values of refractive indices and birefringence in DNA films vary considerably depending on the film fabrication method, solution concentration, drying conditions, and relative humidity of the environment.

The refractive indices of DNA films decrease with increasing humidity in ambient air. Prism coupler measurements show a varying degree of optical anisotropy of films. A high negative birefringence, about -0.03 at an RH ~ 55 %, in the solution cast films, indicates that DNA molecules are highly aligned in a plane parallel to the film surface. However, this alignment changes with humidity. The birefringence almost disappeared at an RH ~ 37%. This might suggest a transition to a different phase, a change in orientation or a change in shape of the molecules.

An almost isotropic DNA polymer film, made by spin deposition, of a more concentrated solution (3 wt % DNA) had a slightly positive birefringence. This suggests that the molecules were randomly orientated. We see a fluctuation in the birefringence in this film at an RH ~ 53-55 %, indicating a change in its molecular organization.

We are keen to rationalize the fluctuations in the optical data in a view of polymorphism and liquid crystalline forms of DNA. The polymer may form mesoscopic liquid crystalline phases during the process of densification of a solution by solvent evaporation and formation of a solid film. The difference in optical anisotropy of the cast and spin-

coated films might have origin in a different speed of solvent evaporation and a concentration-dependent freedom of alignment of the DNA molecules. The humidity-dependent fluctuations of the birefringence indicate a change in the local structure and organization of DNA molecules in moisture-swollen solid films.

3. COMPLEX NONLINEAR REFRACTIVE INDEX OF DNA[32]

It is important to critically evaluate those parameters which may be relevant for photonic device applications of DNA itself and the materials obtained from it and to understand ways in which these parameters can be controlled and modified according to the device requirements. Of special interest is the fact that DNA is chiral and thus it also possesses nonlinear chirooptic properties [33, 34] and can impart chirality on intercalating dyes which can be strong second-order or third-order nonlinear optical chromophores. In the investigation of such nonlinear effects it is necessary to know the parameters of the host material. We present here results of measurements carried out to determine cubic nonlinear optical properties of DNA which are fundamental for evaluation of the properties of waveguiding structures containing DNA-based materials.

3.1 EXPERIMENTAL

The salmon based DNA investigated in our study was the same material as that used in other work [1, 2]. The weight average molecular weight MW of the DNA used was 8×10^6 Daltons (g/mol). This corresponds to 12.1×10^3 nucleotide base pairs (the average molecular mass of the nucleotide base pair is assumed to be 662 g/mol). To characterize the material, we studied the absorption spectra of DNA dissolved in deionized water. The UV absorption peak listed in literature for double-stranded DNA (from bacteria) in H_2O solutions at neutral pH, has λ_{max} at 260 nm, the molar absorption coefficient $\varepsilon = 6.6 \times 10^3$ M^{-1} cm^{-1}, and the specific absorption coefficient is 20 $(mg/ml)^{-1}$ cm^{-1} = 0.020 $(\mu g/ml)^{-1}$ cm^{-1}.[4]

The aqueous (pH 6-6.5) solutions of DNA were prepared at room temperature, 21°C, by dissolving the fiber-like solid material in deionised water. The maximum concentration of DNA was 3 wt %. The solutions were prepared using a typical

procedure in which the components were placed in a glass vial, the vial was closed with a PTFE-lined cap, and placed on a rotating wheel for at least 24 hours to ensure homogenization. UV-visible absorption spectra of the solute of various concentrations were measured in a fused quartz cell with a 1 mm path length with a UV-VIS-NIR spectrophotometer (Shimadzu, model 3101PC).

Figure 5 shows an example absorption spectrum measured in an aqueous solution of DNA.

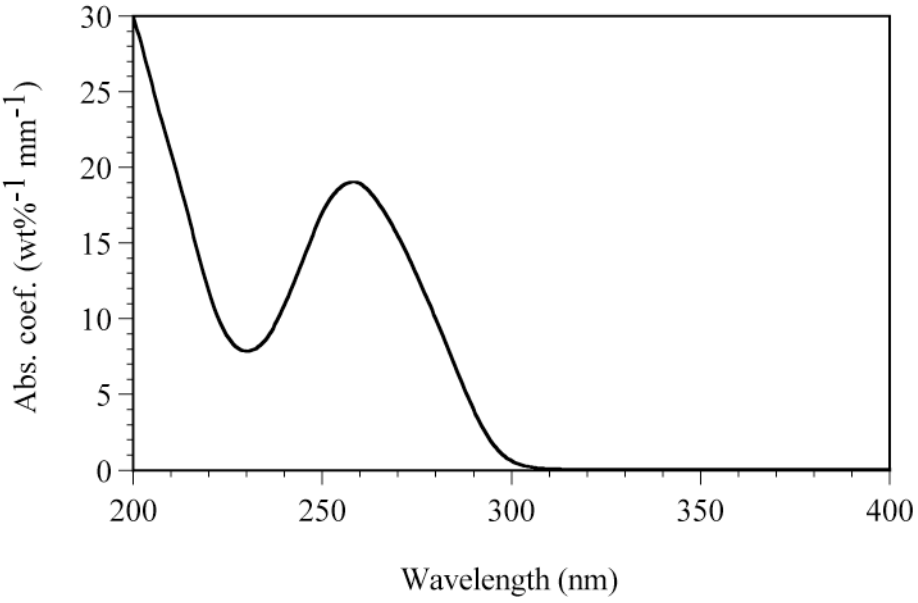

Figure 5 The UV absorption spectrum of a solution of salmon DNA in deionised water at the concentration of 0.0837 wt%, 1mm thick cell. The average value of the specific absorption coefficient for DNA solutions is 18.1 ± 0.7 $(mg/ml)^{-1}$ cm^{-1}, the molar absorption coefficient is (6.0 ± 0.2) x10^3 $M^{-1}cm^{-1}$ at λ_{max} = 258 nm.

We used the Z-scan technique [35] to determine the dispersion of the complex cubic nonlinear susceptibility (related to the nonlinear refractive index n_2 and the two-photon absorption coefficient β_2) in the range of wavelengths 530-1300 nm. These experiments were performed on water solutions of DNA using ~150 fs pulses emitted from an amplified femtosecond laser system, using a Clark MXR CPA-2001 regenerative amplifier, pumping a Light Conversion TOPAS optical parametric amplifier. The system was tuned to wavelengths in the required range using the signal, the doubled idler, the

doubled signal and the idler-pump frequency mixing for four different ranges of the operation of the TOPAS. The repetition rate was kept at 250 Hz for all measurements.

The spot size w_0 was in the range of 30 – 60 μm for various wavelengths and the light intensity was adjusted to keep the nonlinear phase shift ΔΦ typically in the range 0.5-1.0 rd for the cell with the DNA solution. As discussed elsewhere [36, 37], Z-scan measurements on solutions provide a convenient way of determining both the refractive and absorptive part of the complex cubic optical nonlinearity of the solute, provided that sufficiently high concentrations of the solute can be prepared. Assuming additivity of the nonlinear contributions from the solvent and the solute, one can write the complex nonlinear refractive index of a solution as $\hat{n}_{2,solution} = (1-g)\hat{n}_{2,solvent} + g\hat{n}_{2,solute}$ where g is the solute content in the solution and $\hat{n}_2$ denotes the complex nonlinear refractive index.

In order to obtain information on the nonlinear refractive index of the solute we perform, Z-scan experiments on cells with the DNA solutions, as well as on identical cells with the pure solvent (water) and on fused silica samples. The latter is helpful in uniform calibration of the nonlinear index data since the possible inaccuracies of measuring the light intensities at various wavelengths (which involves measurements of pulse power, pulse duration and the focused spot size) are then avoided. Numerical fitting of Z-scan curves provided the values of the real and imaginary parts of the complex nonlinear phase shifts $\Delta\hat{\Phi}$ which could then be used to calculate the real and imaginary parts of the complex nonlinear index $\hat{n}_2$ of the solutions. The phase shifts obtained from measurements on solutions placed in glass cells always include contributions from the glass walls of the cells, but these contributions are eliminated when computing the nonlinearity of the solute by the following relations

$$n_{2,solute,real} = \frac{1}{g}\frac{\Delta\Phi_{real,solution} - \Delta\Phi_{real,solvent}}{\Delta\Phi_{silica}}\frac{L_{silica}}{L_{solution}}n_{2,silica}$$

and

$$n_{2,solute,imag} = \frac{1}{g}\frac{\Delta\Phi_{imag,solution}}{\Delta\Phi_{silica}}\frac{L_{silica}}{L_{solution}}n_{2,silica}$$

where L_{silica} and $L_{solution}$ are the path lengths in the silica standard and in the solution cell. Thus, by comparing the solution results with those for pure solvent (water) we obtain the

extrapolated real and imaginary parts of $\hat{n}_2$ for pure DNA, assuming that the solvent and the cuvette walls do not show nonlinear absorption, which is justified in the range of wavelengths and light intensities used. In the computations we neglected the wavelength dependence of nonlinearity of the standard, assuming the nonlinear refractive index $n_{2,silica}=3x10^{-16}$ cm^2/W over the whole range of the wavelengths.

3.2. RESULTS

As shown in Figure 6 we find that the nonlinear refractive index of DNA varies in the range appr. $2x10^{-15}$ to $1x10^{-14}$ cm^2/W from λ = 1300 nm to 530 nm, respectively. The nonlinear refractive index of water (the solvent) measured against the n_2 of silica was estimated to be in the range 0.5-$1x10^{-15}$ cm^2/W. The range of n_2 values determined for DNA corresponds roughly to the real part of $\chi^{(3)}(-\omega;\omega,-\omega,\omega)$ varying between $8x10^{-14}$ esu and $5x10^{-13}$ esu. The increase of n_2 is accompanied by the appearance of a trace of two-photon absorption at the shortest wavelengths (below λ = 600 nm) which is manifested in Fig. 2 as a slight increase of the imaginary part of $\hat{n}_2$. The latter parameter can be converted to the nonlinear absorption coefficient β_2. We find that β_2 reaches about 0.2 cm/GW at 530 nm, thus, moderate two-photon absorption is possible in DNA at the wavelengths corresponding to twice the wavelength of the position of the main one-photon absorption peak (it should be noted that two-photon absorption cross sections of nucleotides were investigated at λ = 532 nm previously; see [38]).

Considering large errors in the determination of the nonlinear parameters of DNA from solution data (due to the limitation in the accessible concentrations of the DNA solutions), the interpretation of the dispersion of the nonlinear parameters can only be considered preliminary at this stage. We have attempted to model the dispersion with a simple expression for the complex nonlinear refractive index. Similarly to the case described in [39] we used a strategy of a numerical fit of the complex nonlinear index with the equation

$$\hat{n}_2 = \left[\frac{A}{\nu_a - 2\nu - i\Gamma_1} + \frac{B}{\nu_b - 2\nu - i\Gamma_2} \right] \times \frac{1}{\left(\nu_a - \nu - i\Gamma_1\right)^2}$$

where A and B are constants, ν_a and ν_b are frequencies of two transitions and Γ_1 and Γ_2 are the damping constants. Thus, we use here the same set of parameters to describe both the refractive and absorptive optical nonlinearity of DNA. The fit parameters of this equation, represented by the lines in Fig.6, were found to be as follows: the resonant frequencies are ν_a=41900 cm^{-1} and ν_b=50000 cm^{-1}, the damping constants are Γ_1=350 cm^{-1} and Γ_2=500 cm^{-1}.

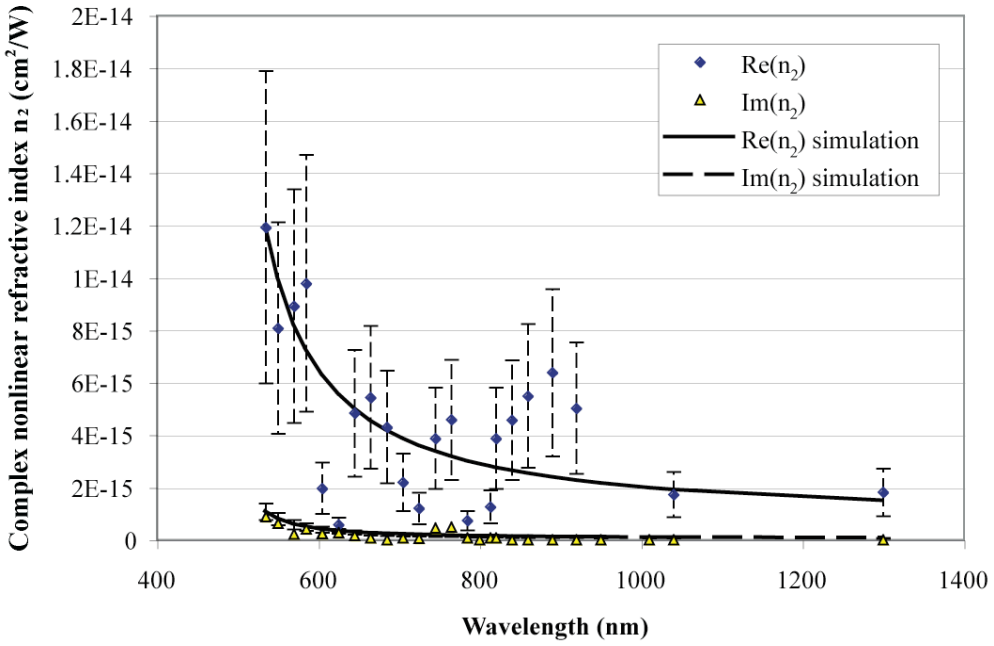

Figure 6 Dispersion of cubic nonlinear optical properties of DNA derived from measurements on water solutions.

We conclude that DNA is a moderately nonlinear photonic material, for which the values of n_2 fall in the range similar to that of typical organic polymers. Apart from the cubic optical nonlinear effects the knowledge of $\chi^{(3)}$ of DNA will also be useful for understanding the second-order nonlinear optical effects in this material (like second harmonic generation and the electrooptic effects) as those may contain components due to the combination of external electric fields with the cubic nonlinearity.

It should be noted that the present study was carried out on native (sodium salt) DNA, not on a surfactant cetyltrimethylammonium counterion substituted DNA (DNA-CTMA), and chromophore containing materials used in many other studies[23].

4. NONLINEAR CHIROOPTIC STUDIES ON INTERCALATED DNA[40]

Nonlinear optical absorption and refraction are commonly known to depend on the polarization of the interacting photons (see e.g. [41]), however, relatively little attention has been given so far to the fact that this polarization sensitivity is present even in the case of the nonlinear optical interactions taking place in isotropic systems like glasses or liquid solutions. The most common cases which necessitate the awareness of and control of the polarization of interacting photons are when two or more beams of light are simultaneously present (as in pump-probe or four-wave mixing interactions), but the single-beam interaction with an isotropic medium is also polarization dependent. These dependences are especially interesting in the case of chiral media: important for biophotonics[34, 42]. Studies of polarization dependent nonlinearities can lead to establishing new techniques for nonlinear imaging, detection of specific molecular structures and understanding of microscopic mechanisms of nonlinear processes.

In the two cases of simple third-order nonlinear optical properties of isotropic media: the nonlinear refraction characterized by the nonlinear refractive index n_2 defined by:

$$\Delta n = n_2 I$$

and the nonlinear absorption characterized by the coefficient β_2 defined by:

$$\Delta\alpha = \beta_2 I$$

(where α is the absorption coefficient) one needs to consider two kinds of polarization dependences. The first of them is the difference between the value of the nonlinear coefficient for the linear and circular polarization of light and the second is the difference between the values of the coefficients for left-handed and right-handed polarization of

light. We define the relative linear-circular nonlinear birefringence as $2(n_{2,linear}-\langle n_{2,circular}\rangle)/(n_{2,linear}+\langle n_{2,circular}\rangle)$ and the relative linear-circular nonlinear dichroism as $2(\beta_{2,linear}-\langle\beta_{2,circular}\rangle)/(\beta_{2,linear}+\langle\beta_{2,circular}\rangle)$. The triangular brackets in the definitions stand for the average between the right-handed and left-handed circular polarization of light. In fact, both n_2 and β_2 can have different values for different senses of the circular polarization if an isotropic medium is composed of chiral components. Thus, the nonlinear circular birefringence can be defined as $\delta n_{2,circ}= n_{2,right}-n_{2,left}$ and the nonlinear circular dichroism as $\delta\beta_{2,circ}= \beta_{2,right}-\beta_{2,left}$ and their relative counterparts can be defined as $\delta n_{2,circ}/\langle n_{2,circular}\rangle$ and $\delta\beta_{2,circ}/\langle\beta_{2,circular}\rangle$. The nonlinear dichroism can also be expressed in terms of the (orientationally averaged) two-photon absorption cross section σ_2 instead of the macroscopic two-photon absorption coefficient β_2. The relation between these two parameters is:

$$\sigma_2 = \frac{\beta_2}{N}\hbar\omega$$

where N is the concentration of the two-photon chromophores and $\hbar\omega$ is the energy of the photon. Alternately, one can also consider the nonlinear optical properties as deriving from molecular hyperpolarizabilities γ and refer to the macroscopic nonlinear effects as due to the polarization dependences of the real and imaginary parts of the hyperpolarizabilities.

In the following we mostly concentrate on the absorptive nonlinearities. We first recall some relevant theoretical work concerning the polarization effects in two-photon absorption and then present examples of techniques that can be used to study those effects and some representative results.

4.1 THEORETICAL BACKGROUND

Both the nonlinear birefringence and dichroism are effects deriving from tensor properties of the nonlinear susceptibilities or the microscopic hyperpolarizabilities in interaction with appropriate field components of the electromagnetic field. The microscopic origin of the nonlinear dichroism is well described in the literature. The

linear-circular nonlinear dichroism is a generally occurring phenomenon explainable in terms of symmetry properties of the sum-over-states expressions describing two-photon absorption. According to Monson and McClain[43], two-photon absorption in a system in which chromophores are randomly oriented can be described by performing averaging of the appropriate product of orientation cosines. The effective two-photon cross section can be obtained for the case of the two electromagnetic field polarization vectors $\boldsymbol{\lambda}$ and $\boldsymbol{\mu}$ describing the two photons being absorbed (of the same or different energies). Defining polarization variables F, G and H as:

$$F = 4\,|\boldsymbol{\lambda}\cdot\boldsymbol{\mu}|^2 - 1 - |\boldsymbol{\lambda}\cdot\boldsymbol{\mu}^*|^2$$

$$G = -\,|\boldsymbol{\lambda}\cdot\boldsymbol{\mu}|^2 + 4 - |\boldsymbol{\lambda}\cdot\boldsymbol{\mu}^*|^2$$

$$H = -\,|\boldsymbol{\lambda}\cdot\boldsymbol{\mu}|^2 - 1 + 4\,|\boldsymbol{\lambda}\cdot\boldsymbol{\mu}^*|^2$$

one can present the effective cross section $\langle\sigma_2\rangle$ obtained at the combination of photon polarizations given by the F, G and H triple as

$$\langle\sigma_2\rangle = \sigma_F F + \sigma_G G + \sigma_H H$$

where

$$\sigma_F \propto |S_{\alpha\alpha}|^2 \qquad \sigma_G \propto S_{\alpha\beta}\,S_{\alpha\beta} \qquad \sigma_H \propto S_{\alpha\beta}\,S_{\beta\alpha}$$

and $S_{\alpha\beta}$ stand for the components of the molecular sum over states:

$$S_{\alpha\beta} = \sum_i \left(\frac{L_\alpha^i M_\beta^i}{k_i - k_\lambda} + \frac{L_\beta^i M_\alpha^i}{k_i - k_\mu} \right)$$

where L and M are transition moments, k_i is the transition state energy and k_λ and k_μ are photon energies.

For two identical photons, both of them linearly polarized along the x laboratory axis and propagating along z: $\lambda = \mu = (1,0,0)$; (F,G,H) = (2,2,2) and accordingly $\langle\sigma_2\rangle = 2\sigma_F + 4\sigma_G$ ($\sigma_G = \sigma_H$ for two same energy photons). For two circularly polarized photons copropagating along z, $\lambda = \mu = (1/2)^{1/2}(1,-i,0)$; (F,G,H) = (-2,3,3) thus $\langle\sigma_2\rangle = -2\sigma_F + 6\sigma_G$. The linear-circular nonlinear dichroism is therefore predicted in terms of molecular properties and it may be a useful indicator of the symmetry properties of the two-photon absorption active excited states.

The other effect considered here is the nonlinear circular dichroism. The circular dichroism is not present in the dipolar approximation used above and its rigorous introduction requires extension of the Monson and McClain model. Such an extension was presented by Tinoco in his 1975 paper[44]. The difference between the σ_2 values obtained for the simplest case when two photons of the same circular polarization are propagating in the same direction is given by the equation:

$$\sigma_L - \sigma_R = \frac{(2\pi)^4 \nu^2 g(2\nu)}{(hc)^2} \frac{4}{15} \left[b_1 \alpha_{0f}^{\mu m} : \alpha_{0f}^{\mu\mu} + b_2 \frac{\pi\nu}{c} \alpha_{0f}^{\mu Q} : \alpha_{0f}^{\mu\mu} + b_3 \alpha_{0f}^{\mu m} \alpha_{0f}^{\mu\mu} \right]$$

where the three polarizabilities α_{0f} with different upper indexes are calculated taking into account the dipolar (μ), magnetic (m) and quadrupole (Q) transitions as defined in Tinoco's paper. The coefficients b_1, b_2 and b_3 have the same role as F, G and H in Monson and McClain's paper, i.e. they depend on the polarization of the two interacting photons. They do depend also on the direction of propagation. For two copropagating left circularly polarized photons $(b_1,b_2,b_3) = (6,2,-2)$. We note that Tinoco's formalism was recently used by Jansik et al[45] to compute two-photon circular dichroism of tryptophan

and tyrosine thus there is potential for comparing the experimental results with theoretical predictions.

4.2 POLARIZATION-MODULATED Z-SCAN

We have suggested in a previous paper[33] that polarization dependences of the nonlinear refraction and nonlinear absorption may be conveniently studied with a number of techniques based on Z-scan. A polarization-modulated Z-scan was shown to be a useful tool for simultaneous recording of the absorptive and refractive components of the nonlinearity as well as their polarization dependences. The idea of investigating polarization dependences by Z-scan was already used by DeSalvo et al[46] who measured anisotropy of nonlinearities for crystalline samples and by Egorov et al[47] who compared nonlinear absorption results for linear and circular polarization for solutions of nonlinear chromophores.

In our implementation of polarization-modulated Z-scan a rotating quarter-wave plate is used to modulate the polarization and signals are recorded at various harmonics of the rotation frequency[33]. For a quarter-wave plate positioned at an angle ϕ to the zero position the Jones matrix can be written as

$$M(\phi) = e^{i\pi/4}\begin{pmatrix}\cos\phi & -\sin\phi\\ \sin\phi & \cos\phi\end{pmatrix}\begin{pmatrix}1 & 0\\ 0 & i\end{pmatrix}\begin{pmatrix}\cos\phi & \sin\phi\\ -\sin\phi & \cos\phi\end{pmatrix}.$$

Thus,

$$M(\phi) = e^{i\pi/4}\begin{pmatrix}\cos^2\phi + i\sin^2\phi & (1-i)\sin\phi\cos\phi\\ (1-i)\sin\phi\cos\phi & \sin^2\phi + i\cos^2\phi\end{pmatrix}$$

so, using a laser polarized along x, the photon polarization after the quarter-wave plate is $\boldsymbol{\lambda}(\phi) = \boldsymbol{\mu}(\phi) = e^{i\pi/4}\left(\cos^2\phi + i\sin^2\phi, (1-i)\sin\phi\cos\phi, 0\right)$. The polarization changes from linear at ϕ=0 to circular at ϕ=π/4, $\boldsymbol{\lambda}(\pi/4) = \boldsymbol{\mu}(\pi/4) = e^{i\pi/4}\left(1/2 + i/2, 1/2 - i/2, 0\right)$; the same linear polarization again at π/2, inverse sense circular at 3π/4, $\boldsymbol{\lambda}(3\pi/4) = \boldsymbol{\mu}(3\pi/4) =$

$e^{i\pi/4}\left(1/2+i/2,\ -1/2+i/2,\ 0\right)$; back to linear at π etc. It follows that any changes of the signal due to circular-linear dichroism and birefringence appear with a period of $\pi/2$ while those due to circular dichroism and birefringence have the period of π. The principle of the experiment is thus that one can simultaneously measure the usual Z-scan aperture transmitted power $P_0(z)$ and its modulation at the second and fourth harmonics of the quarter-wave rotation frequency $P_{2\Omega}(z)$ and $P_{4\Omega}(z)$ and relate those to the polarization dependences of the nonlinear effects.

One can assume that, within a certain range of values, transmission changes seen in closed-aperture or open-aperture Z-scans are proportional to the values of the appropriate nonlinear coefficients. Taking as an example the open-aperture signal due to two-photon absorption, the transmission change measured in the system with a rotating quarter-wave plate averaged over all orientations of the plate can be defined as $\Delta P_0=P_0(z=0)-P_0(z>>z_R) \propto (\sigma_{2,linear}+<\sigma_{2,circular}>)/2$. The modulation signals arise because of the variation of the transmission with polarization. Ideally, the value of transmission at low intensity, i.e. for the sample being far from the focal plane $P_0(z>>z_R)$ should not be polarization dependent and the modulation signal should be zero there, however, in practice there may be residual signals due to optical (e.g. one-photon circular dichroism) and electrical (e.g. pickup) sources. For the fourth-harmonic modulation amplitude we find that the signal at z=0 should oscillate with the angle ϕ, between the value for the absorption of linearly polarized beam and that for a circularly polarized beam, thus $\Delta P_{4\Omega}=P_{4\Omega}(z=0)-P_{4\Omega}(z>>z_R) \propto (\sigma_{2,linear}-<\sigma_{2,circular}>)/2$. The relative linear-circular dichroism of the two-photon absorption signal is thus determined in the following manner:

$$\kappa_4 = \frac{\Delta P_{4\Omega}}{\Delta P_0} = \frac{\sigma_2^{lin} - \sigma_2^{circ}}{\sigma_2^{lin} + \sigma_2^{circ}} = \frac{2\sigma_F - \sigma_G}{\sigma_G}$$

In terms of the tensor components of $S_{\alpha\beta}$ this translates to:

$$\kappa_4 = \frac{2\sum_{\alpha} |S_{\alpha\alpha}|^2 - \sum_{\alpha}\sum_{\beta} S_{\alpha\beta}\bar{S}_{\alpha\beta}}{5\sum_{\alpha}\sum_{\beta} S_{\alpha\beta}\bar{S}_{\alpha\beta}}$$

In a similar way, the signal recorded at the second harmonic of the quarter-wave rotation should be related to the nonlinear circular dichroism and will be given by

$$\kappa_2 = \frac{\Delta P_{2\Omega}}{\Delta P_0} = \frac{\sigma_{2,L}^{circ} - \sigma_{2,R}^{circ}}{\sigma_2^{lin} + \sigma_2^{circ}} = \frac{\sigma_L - \sigma_R}{2 < \sigma_2 >_{l-c}}$$

4.3 THERMAL LENSING DETECTED TWO-PHOTON ABSORPTION

There are several difficulties in implementing polarization-dependent Z-scan. Among them one needs to list the inherently poor signal-to-noise ratio when carrying out experiments with low repetition rate amplified femtosecond laser systems. In the following we consider polarization effects on two-photon absorption as investigated by the technique of thermal lensing detected absorption of a mode-locked laser beam. This technique appears to be suitable for investigations of two-photon absorption in liquid solutions of two-photon chromophores, in particular, it is applicable to chromophores that are not strong fluorophores and thus are not conveniently studied by the two-photon induced fluorescence technique (e.g. [48]). We have performed tests of the use of the two-photon induced fluorescence in conjunction with the Z-scan principle and with polarization modulation using a rotating quarter-wave plate. Signals that could be attributed both to the linear-circular two-photon dichroism (fourth-harmonic signals) and to the circular two-photon dichroism (second-harmonic signals) were detected. Those results will not be, however, discussed in the present paper.

The principle of the thermal lensing experiments is illustrated in Figure 7.

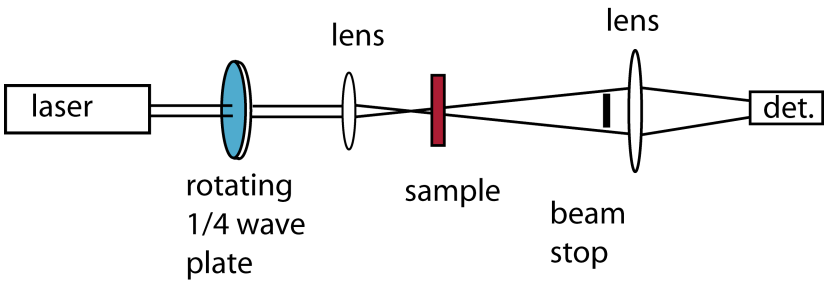

Figure 7 The principle of thermal lensing-detected polarization dependent two-photon absorption measurements.

The beam from a mode-locked laser source is passed through a rotating quarter-wave plate and then focussed with a lens. The sample (typically a solution of a chromophore in an organic solvent placed in a 1 mm glass cell) can be positioned at different distances, z, from the focal plane, as in Z-scan measurements[35]. After passing through the sample, the central part of the beam is blocked by a beam stop in form of a disk, thus only its perimeter part is collected by a large diameter lens and focused on a detector. This signal detection setup is thus identical to the so-called EZ-scan technique (eclipsed Z-scan)[49] combined with the polarization modulated Z-scan[33]. The principle of its operation is the detection of two-photon absorption by its accompanying thermal effect. For the sample positioned close to the focal plane (z=0), the heat deposited through the two-photon absorption process causes the appearance of a self-defocussing effect (since the thermal-induced change of the refractive index in an organic solvent is, as a rule, negative). This either decreases (for the sample at $z<0$) or increases (for $z>0$) the transmission of the system. As discussed by Xia et al[49], the sensitivity of detection of the nonlinear effect is dependent on the degree of obscuration of the beam by the disk, the sensitivity being higher for a lower transmission.

The detector signal is fed into an A/D converter and collected by a computer synchronously with the rotation of the quarter-wave plate. The frequency components of the signal are calculated by the computer using a digital lock-in principle. The various harmonics $P_{n\Omega}$ (measured in our system up to the eighth, n = 0 to 8) are given by the relation:

$$P_{n\Omega} = \frac{1}{s}\sum_{i=1}^{s} P(i)\sin(2\pi n\frac{i}{s})$$

where s is the number of steps for a complete rotation.

The thermal lensing detection was used to demonstrate feasibility of measuring two-photon absorption in non-fluorescent dyes on an example of Disperse Red 1 (DR1). Disperse Red 1 was investigated in two different environments: as a solution of the dye in n-butanol and as a solution in n-butanol containing also 4% of deoxyribonucleic acid treated with CTMA surfactant (DNA-CTMA)[2, 50]. Clearly, the first of the solutions contains a random collection of DR1 molecules while the DR1-DNA-CTMA system is more complicated because of the intrinsic chirality of DNA chains which also imposes chirooptic properties onto the dye which, to some extent, may be intercalating the DNA chains or binding to them in another manner.

Figure 8 shows examples of EZ-scans obtained on the two solutions of DR1 using ~200 mW average power at 800 nm from a mode-locked femtosecond Ti-sapphire laser system (Coherent Verdi-pumped Mira 900D laser) with ~150 fs pulses.

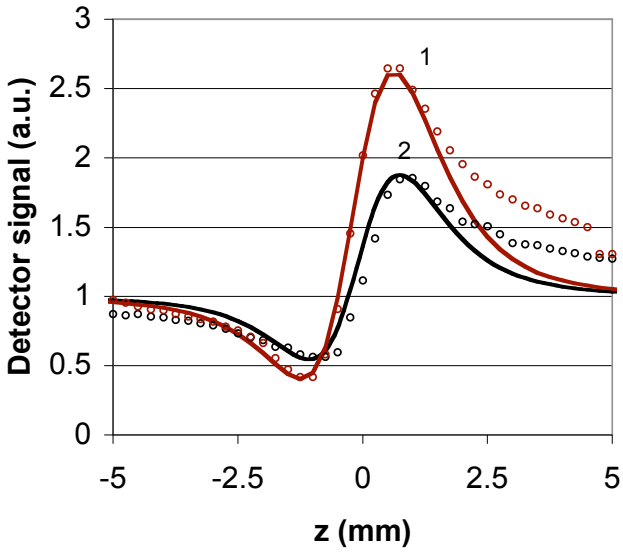

Figure 8 Eclipsed Z-scans obtained on two samples of DR1 solutions: a 5% solution in n-butanol (curve 1) and a 2.8 % of DR1 in solution in butanol together with

4% of DNA-CTMA (curve 2). The full lines are curves computed from Z-scan theory[35] by direct integration of the intensity profile at the plane of the beam blocking disk. The fitted parameters are $w_0 = 18.5$ μm, transmission = 15%, $\Delta\phi_0 = -1.75$ rd (curve 1) and –1.1 rd (curve 2)

As expected, the EZ scans show a distinctive pattern of a valley followed by a peak which is indicative of a negative refractive nonlinearity ($n_2 < 0$). There is no doubt that this nonlinear effect originates from thermal nonlinearity. Since the repetition rate of a mode-locked laser (86 MHz) is much higher than the inverse of the typical relaxation time of the thermal effect in solution (ms range), the effective thermal nonlinearity can be treated in the same way as for a cw beam. From the relation $\Delta\phi_0 = 2\pi n_2 I \frac{L}{\lambda}$ the effective n_2 for the two samples in Fig. 3 is found to be 5.7×10^{-9} and 3.6×10^{-9} cm^2/W, respectively, which approximately scales with the concentration of DR1 in the two solutions. As will be shown below, these values can, in principle, be used to calculate outright the two-photon absorption coefficient for DR1, however, due to numerous uncertainties concerning the beam parameters and the particulars of the thermal nonlinear process, such a calculation can only be considered an order-of-magnitude approximation and more precise values should be obtained by comparison with solutions of standard chromophores of known two-photon absorption properties. An estimate of the two-photon absorption coefficient can be made from the equation for effective thermally induced n_2 given in [37, 51] for the case of one-photon absorption:

$$n_{2,eff}(\omega, s) = \left[\left(\frac{\partial n}{\partial T} \right)_V - \frac{n^2 - 1}{2n} \beta \right] \frac{\alpha}{i\omega c_p \rho + s^2 \kappa}$$

where ω is the frequency and s is the spatial frequency of illumination, β is the volume expansion coefficient, α is the absorption coefficient, c_p is the specific heat, ρ is the density and κ is the heat conductivity coefficient. Under the conditions of a mode-locked train a cw approximation can be used (ω= 0) and one can assume that the only absorption

process is that due to two-photon absorption and the refractive index change is only due to volume expansion. One gets then:

$$n_{2,eff}(0,s) = -\frac{n^2-1}{2n}\beta\,\frac{\beta_2 I_{peak}}{s^2\kappa}$$

which indicates that the effective nonlinear refractive index depends on the peak intensity of the fs pulses (which is not surprising: one expects that the amount of heat deposited in a two-photon absorption process depends on the square of the peak intensity) and on the square of the spatial frequency (which we approximate here as $s=1/w_0$). Taking n=1.40, $\beta = 1.3\times10^{-3}$ K^{-1}, $\kappa=1.5\times10^{-3}$ W/cmK (CRC Handbook) we get $\beta_2 I_{peak}=5.6\times10^{-3}$ cm^{-1}. The peak intensity can be estimated as 3 GW/cm^2, thus $\beta_2=1.9\times10^{-12}$ cm/W and the two-photon cross section for DR1 is evaluated as 0.6×10^{-50} cm^4s (0.6 GM). This is not very different from σ_2=2.8 GM derived from the direct open-aperture Z-scan measurement at 775 nm by De Boni[52] and our own unpublished data, in both cases obtained with amplified femtosecond systems.

Potentially, the technique used by us here may become a useful tool for investigating nonlinear absorption, especially if reliable standards are used for calibrating the measurement. However, the present implementation of the thermal lensing detection is mostly targeting the polarization effects in nonlinear absorption.

Figure 9 shows data obtained by modulating polarization on the sample of DR1 dissolved in butanol containing DNA-CTMA. The Fourier components obtained at the second and fourth harmonic of the rotation frequency of the quarter-wave plate are here normalized by dividing their values by the dc component (the zeroth harmonic) of the EZ-scan signal measured far from the focal plane $P_0(z>>z_R)$. These components are plotted as the function of the input power for two positions of the sample: that corresponding to the maximum of the EZ-scan curve and that corresponding to the minimum of the curve. As mentioned before, the thermal lensing detected two-photon absorption signal is expected to be proportional to the square of the peak intensity of the

input beam, thus the normalized modulation signals plotted in Figure 4 are expected to be linearly dependent on the input power. Indeed, approximately linear dependences are seen, with the slopes of the lines being reversed between the data obtained for the maximum and the minimum of the EZ-scans. It can be concluded that both the linear-circular nonlinear dichroism and the nonlinear circular dichroism are observed in this type of a sample. The magnitudes of these effects can be estimated from the results presented in Fig.9.

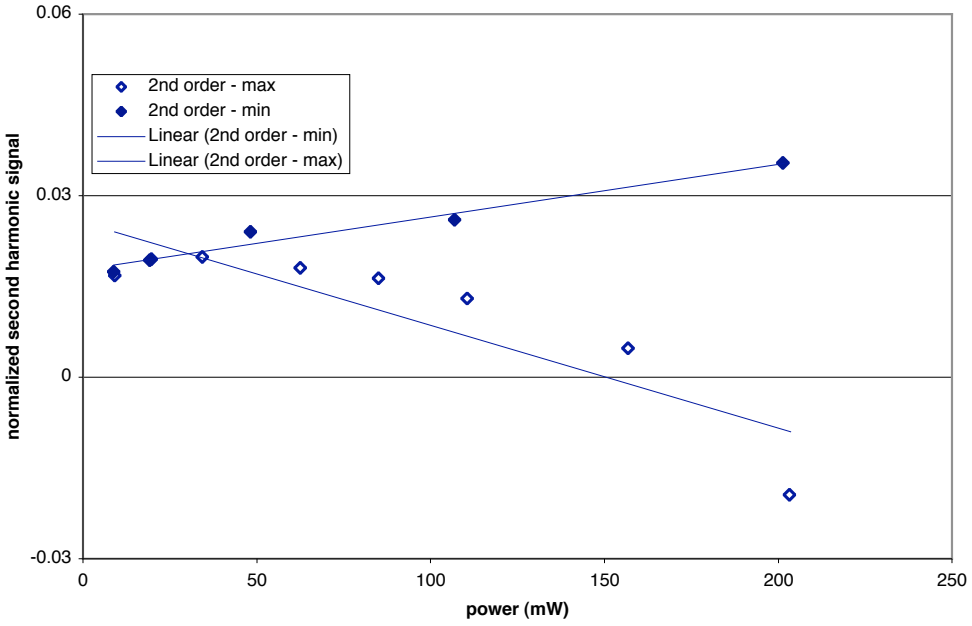

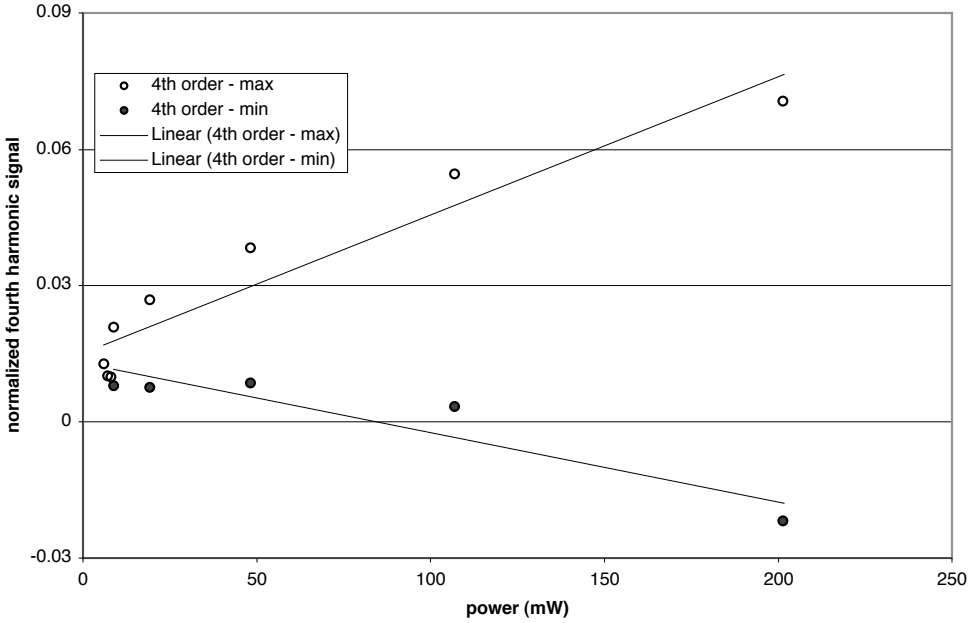

Figure 9 Polarization modulation signals for a sample of DR1-DNA-CTMA in butanol. Full symbols denote data obtained at the maximum of the EZ-scan curve, open symbols denote data for the EZ-scan curve minimum.

The results are listed in Table 2 together with the data obtained for DR1 solution in butanol without the DNA

Table 2 Comparison of polarization modulation of the two-photon absorption in DR1 and DR1-DNA-CTMA

Sample	DR1	DR1 + DNA-CTMA
Modulation at 4^{th} harmonic κ_4 (%)	1.4 ± 0.2	7.6 ± 0.8
Modulation at the 2^{nd} harmonic κ_2 (%)	$< 0.67 \pm 0.4$	$- 4.1 \pm 0.7$

Figure 10 illustrates the modulation for rotating quarter-wave plate in the case of DR1+DNA-CTMA.

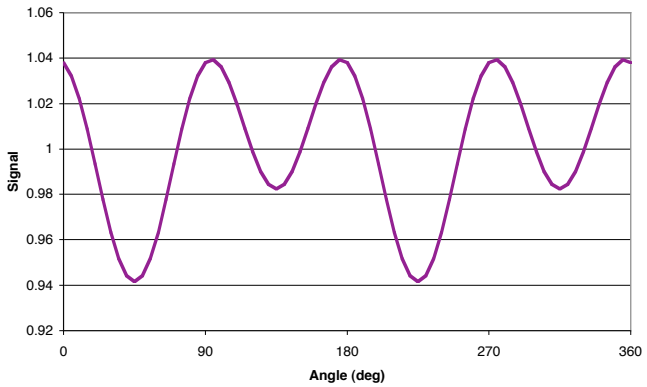

Figure 10 The recovered modulation of the two-photon signal at 200mW power for DR1+DNA-CTMA solution

Interestingly, the modulation effects are in all cases distinctly observable with an exception of the κ_2 effect for neat DR1 solution which is within the experimental spread of the results essentially nonexistent. This is what was expected, because the κ_2 effect, due to circular dichroism, should be absent in DR1 solutions. Other effects are all well in excess of 10^{-2} and above the experimental scatter. However, a warning must be made concerning possible causes of spurious signals appearing at the second and fourth harmonic of the rotation frequency. The lines in Fig.9 do not have zero intercept which indicates that some modulation of the transmission takes place at low powers: obviously not due to the two-photon absorption process. This is similar to the background modulation signal which was observed in polarization-modulated Z-scans even for $z>>z_R$. In addition, there are also deviations of the signals from the straight-line behaviour which appear especially at higher powers. For the current series of measurements such deviations were particularly noticeable for powers above 200 mW possibly due to noise caused by excessive temperature increase in the focal region of the beam (it is not uncommon to see boiling of an absorbing solution when investigated by Z-scan like techniques under cw illumination or with long pulses).

However, the results in Table 1 indicate that the nonlinear optical properties of the DR1 dye do become modified through the interactions with DNA and that polarization dependent two-photon absorption may be a useful technique for investigating such interactions.

4.4 CONCLUSIONS

Polarization-modulated cubic and higher-order nonlinearities offer a rich field of studies. Linear-circular two-photon dichroism effects on the order of several percent are observed in several cases. In particular, linear-circular dichroism of two-photon absorption may be a useful contrast mechanism in microscopy.

5. DYNAMIC HOLOGRAPHICALLY WRITTEN GRATINGS IN DNA-CTMA:DR1

DNA-based biopolymer used in this research was fabricated from the salmon roe DNA by first purifying it and then complexing with a cationic surfactant, cetyltrimethyl-ammonium (CTMA) chloride according to procedure described by Heckman et al.[3] and Wang et al[23]. In DNA-CTMA the sodium ions are replaced with cetyltrimethyl-ammonium ions enabling its solubility in several organic solvents including 1-butanol, which was used here for sample preparation. We prepared a butanol solution of DNA-CTMA and DR-1 to obtain a 4 % solution of DR1 in DNA-CTMA in a dry form. It should be stressed that at present we do not know in which way DR1 is bound to DNA. It can lie roughly perpendicular to the DNA helix axis or can be oriented in the major and minor groves of the DNA double helix and lie parallel to the helix axis, or it can be intercalated between the base pairs, however, we believe that different types of binding of the oriented nucleic acid with nonlinear optical dyes may bring new functionalities to DNA.

The absorbance of the film of DR1:DNA-CTMA obtained by casting is shown in Fig. 11.

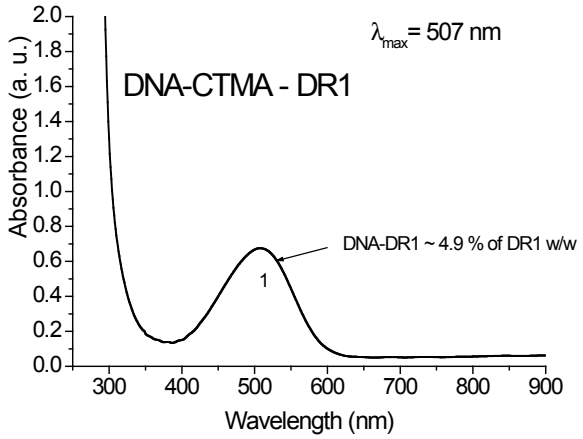

Figure 11 UV-VIS absorption spectra of a DNA-CTMA:DR1 film deposited on glass substrate.

The film was then placed between two ITO covered glass plates and sealed in order to prevent optically induced oxidation, which degrades the nonlinear optical properties of azobenzene derivatives.

Experimental set-up for holographic grating recording and diffraction efficiency measurements is shown in Fig. 2. Polymeric sample is set at normal position to bisectrice of Ar^+ laser beam illumination (λ = 488 or 514.5 nm). Both beams are s-s polarized and equal in intensity. Their interference is producing an light intensity pattern on the sample with grating wave-vector $|\vec{q}| = 2\pi / \Lambda$. Angle 2 θ between the incident beams defines the grating period $\Lambda = \dfrac{\lambda}{2\sin(\theta/2)}$. Another laser (He-Ne, (λ = 632.8 nm) illuminates the sample within the grating area and the diffracted into first diffraction order direction light is measured with fast Si calibrated photodiode.

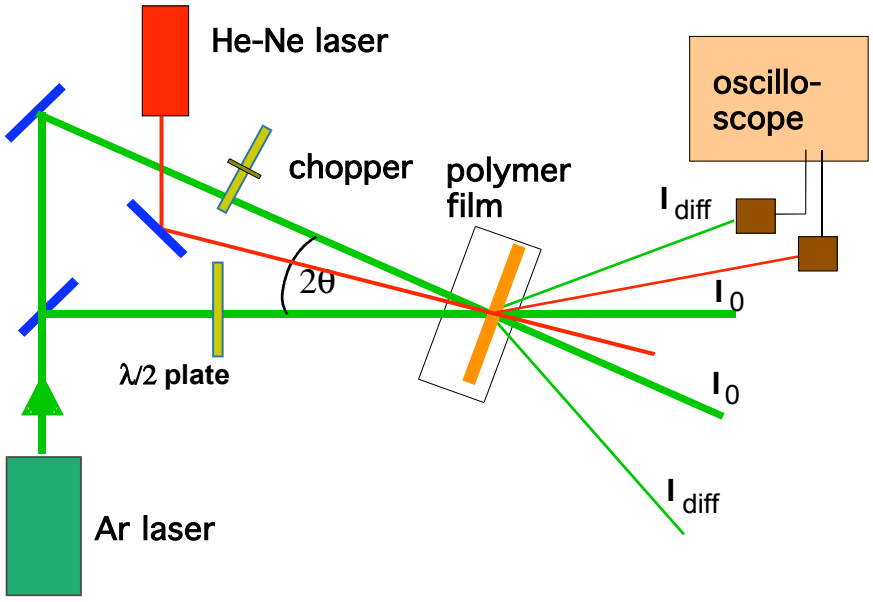

Fig. 12. Experimental setup for holographic grating recording and diffraction efficiency measurements. A λ/2 retardation plate enables polarization grating recording.

Measurements of light self-diffraction were performed using 488 nm and 514.5 nm of cw Ar^+ laser light. The light self-diffraction appears almost instantaneously in the films of DNA-CTMA DR1 and also the grating decay is very fast after light shut off. This finding is important for the field of dynamic holography where materials exhibiting the fast and reversible hologram recording properties are desired. In most azo-functionalized polymers the grating build-up observed in typical two-wave mixing set-up is a slow process with grating growth time constants of the order of seconds to hours. Here we report for the first time, up to our knowledge, the optical grating recording in Disperse Red 1 dye containing DNA-CTMA matrix with an excellent stability and dynamics. In Fig. 13 we present the recording of grating using intensity pattern of 16.45 μm period in thin film of DNA-CTMA DR1. Rectangular shape seen in an oscilloscope trace corresponds to response of detector measuring chopped recording laser (λ = 514.5 nm) beam while another trace corresponds to first order diffraction signal of the remaining laser beam. The presence of this signal and its dynamics is directly related to

diffraction grating build-up and decay in the sample. Notice that the timescale of the plot is in ms range and the signal repeatability is excellent.

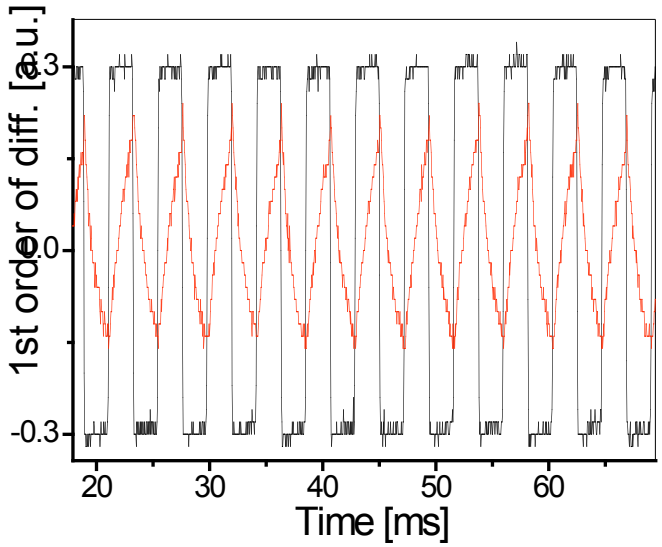

Fig. 13. 1st order self-diffraction signal measured for DNA-CTMA-DR1 in two-wave mixing experiment using λ = 514.5 nm as excitation wavelength and grating period Λ = 16.45 µm. One of the recording incoming beams was chopped. The s-s polarization recording and 130 mW of total laser power at 514.5 nm were used.

In Fig. 14 the shape of the signal is shown for the expanded time scale to few milliseconds. One can assume that for low light intensities (here < 1 W/cm^2) diffraction is mainly due to a *cis-trans* population grating that decays in a millisecond time scale.

These preliminary data show that investigations of dynamic gratings in dye-doped DNA materials may lead to very promising results. Further studies of this phenomenon are currently carried out.

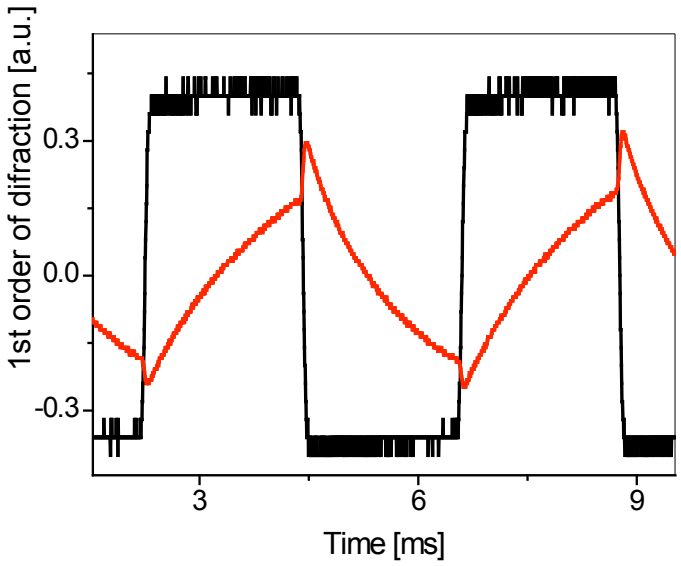

Fig. 14. An example of an oscilloscope trace during dynamic grating recording (one of the recording beams is chopped at frequency 195 Hz – black line) in DNA-CTMA-DR1. Light self-diffraction of Ar^+ laser beam (red curve). Polarization s-s, total power 110 mW at 514.5 nm.

References

1. A. Samoc, A. Miniewicz, M. Samoc, and J. G. Grote, "Refractive Index Anisotropy and Optical Dispersion in Films of Deoxyribonucleic Acid (DNA)," J.Appl.Polym.Sci submitted (2006).
2. J. G. Grote, D. E. Diggs, R. L. Nelson, J. S. Zetts, F. K. Hopkins, N. Ogata, J. A. Hagen, E. Heckman, P. P. Yaney, M. O. Stone, and L. R. Dalton, "DNA photonics (Deoxyribonucleic Acid)," Mol. Cryst. Liq. Cryst. **426**, 3-17 (2005).
3. E. M. Heckman, J. A. Hagen, P. P. Yaney, J. G. Grote, and F. K. Hopkins, "Processing techniques for deoxyribonucleic acid: Biopolymers for photonics applications," Appl. Phys. Lett. **87**, 211115-211111/211113 (2005).
4. D. Freifelder, *Physical Biochemistry,* 2nd ed. (W. H. Freeman and Company, San Francisco, CA, 1982).
5. G. H. Beaven, E. R. Holiday, and E. A. Johnson, "Optical properties of nucleic acids and their components," in *The Nucleic Acids Chemistry and Biology*, E. Chargaff and J. N. Davidson, eds. (Academic Press, New York, 1955), pp. 493-553.
6. W. Saenger, *Principles of Nucleic Acid Structure*, Spinger Advanced Texts in Chemistry (Springer-Verlag, New York, 1984).
7. R. F. Boyer, *Modern Experimental Biochemistry* (Addison-Wesley Publishing Company, Reading, MA, 1986).
8. R. Ulrich and T. R., "Measurement of thin film parameters with a prism coupler," Appl. Opt. **12**(12), 2901-2908 (1973).
9. P. K. Tien, "Integrated optics and new wave phenomena in optical waveguides," Rev. Mod. Phys. **49**(2), 361-420 (1977).
10. N. Morii, G. Kido, H. Suzuki, S. Nimori, and H. Morii, "Molecular chain orientation of DNA films induced by both the magnetic field and the interfacial effect," Biomacromolecules **5**(6), 2297-2307 (2004).
11. S. M. Lindsay, S. A. Lee, J. W. Powell, T. Weidlich, C. Demarco, G. D. Lewen, N. J. Tao, and A. Rupprecht, "The origin of the A to B transition in DNA fibers and films," Biopolymers **27**(6), 1015-1043 (1988).
12. G. Lewen, S. M. Lindsay, N. J. Tao, T. Weidlich, R. J. Graham, and A. Rupprecht, "A mechanism for the large anisotropic swelling of DNA films," Biopolymers **25**(5), 765-770 (1986).
13. A. Kagemoto, M. Nakazaki, S. Kimura, Y. Momohara, K.-I. Ueno, and Y. Baba, "Calorimetric investigation on liquid crystals of deoxyribonucleic acid in concentrated solutions," Thermochim. Acta **284**(2), 309-324 (1996).
14. R. Brandes and D. R. Kearns, "Magnetic ordering of DNA liquid crystals," Biochemistry **25**(20), 5890-5895 (1986).
15. T. E. Strzelecka, M. W. Davidson, and R. L. Rill, "Multiple liquid crystal phases of DNA at high concentrations," Nature **331**(6155), 457-460 (1988).
16. T. E. Strzelecka and R. L. Rill, "Phase transitions of concentrated DNA solutions in low concentrations of 1:1 supporting electrolyte," Biopolymers **30**(1-2), 57-71 (1990).

17. D. H. Van Winkle, M. W. Davidson, W. X. Chen, and R. L. Rill, "Cholesteric helical pitch of near persistence length DNA," Macromolecules **23**(18), 4140-4148 (1990).
18. D. H. Van Winkle, M. W. Davidson, and R. L. Rill, "Terraces in the cholesteric phase of DNA liquid crystals," J. Chem. Phys. **97**(8), 5641-5646 (1992).
19. R. L. Rill, T. E. Strzelecka, M. W. Davidson, and D. H. Van Winkle, "Ordered phases in concentrated DNA solutions," Physica A **176**, 87-116 (1991).
20. A. Leforestier and F. Livolant, "Supramolecular ordering of DNA in the cholesteric liquid crystalline phase: An ultrastructural study," Biophys. J. **65**, 56-72 (1993).
21. F. Livolant, "Supramolecular organization of double-strabded DNA molecules in the columnar hexagonal liquid crystalline phase," J. Mol. Biol. **218**, 165-181 (1991).
22. H. H. Strey, J. Wang, R. Podgornik, A. Rupprecht, L. Yu, V. A. Parsegian, and E. B. Sirota, "Refusing to twist: Demonstration of a line hexatic phase in DNA liquid crystals," Phys. Rev. Lett. **84**(14), 3105-3108 (2000).
23. L. Wang, J. Yoshida, N. Ogata, S. Sasaki, and T. Kajiyama, "Self-assembled supramolecular films derived from marine Deoxyribonucleic Acid (DNA)-cationic surfactant complexes: large-scale preparation and optical and thermal properties," Chem. Mater. **13**(4), 1273-1281 (2001).
24. G. Zhang, L. Wang, J. Yoshida, and N. Ogata, "Optical and optoelectronic materials derived from biopolymer deoxyribonucleic acid (DNA)," Proc. SPIE **4580**, 337-346 (2001).
25. T. Weidlich, S. M. Lindsay, and A. Rupprecht, "The optical properties of Li- and Na-DNA films," Biopolymers **26**(3), 439-453 (1987).
26. P. J. Adams, M. L. VanSteenberg, S. A. Lee, and A. Rupprecht, "Optical properties of CsDNA films as a function of hydration," J. Biomol. Struct. Dynam. **11**(6), 1277-1286 (1994).
27. T. Inagaki, R. N. Hamm, E. T. Arakawa, and L. R. Painter, "Optical and dielectric properties of DNA in the extreme ultraviolet," J. Chem. Phys. **61**(10), 4246-4250 (1974).
28. J. Ulanski, P. Wojciechowski, and M. Kryszewski, "Unconventional anisotropic polymer/crystalline phase composites," Mol. Cryst. Liq. Cryst. S&T, Sect. B: Nonl. Opt. **9**(1-4), 203-211 (1995).
29. P. Wojciechowski, L. Okrasa, J. Ulanski, and M. Kryszewski, "Thermally stable optically anisotropic polymer networks obtained from mesogenic LC cellulose derivatives," Adv. Mater. Opt. Electron. **6**(5&6), 383-386 (1996).
30. M. Kryszewski, "Fifty years of study of the piezoelectric properties of macromolecular structured biological materials," Acta Phys. Polon., A **105**(4), 389-408 (2004).
31. R. Swanepoel, "Determining refractive index and thickness of thin films from wavelength measurements only," J. Opt. Soc. Am. **2**(8), 1339-1343 (1985).
32. M. Samoc, A. Samoc, and J. G. Grote, "Complex nonlinear refractive index of DNA," Chemical Physics Letters submitted (2006).

33. P. P. Markowicz, M. Samoc, J. Cerne, P. N. Prasad, A. Pucci, and G. Ruggeri, "Modified Z-scan techniques for investigations of nonlinear chiroptical effects," Optics Express **12**(21), 5209-5214 (2004).
34. P. Fischer and F. Hache, "Nonlinear optical spectroscopy of chiral molecules," Chirality **17**, 421-437 (2005).
35. M. Sheikh-bahae, A. A. Said, T. Wei, D. J. Hagan, and E. W. v. Stryland, "Sensitive Measurement of Optical Nonlinearites Using a Single Beam," IEEE J. Quantum Electr. **26**, 760-769 (1990).
36. M. Samoc, A. Samoc, B. Luther-Davies, Z. Bao, L. Yu, B. Hsieh, and U. Scherf, "Femtosecond Z-scan and degenerate four-wave mixing measurements of real and imaginary parts of the third-order nonlinearity of soluble conjugated polymers," J. Opt. Soc. Am. B **15**(2), 817-825 (1998).
37. M. Samoc, A. Samoc, B. Luther-Davies, M. G. Humphrey, and M.-S. Wong, "Third-order optical nonlinearities of oligomers, dendrimers and polymers derived from solution Z-scan studies," Optical Materials, **21**(1-3), 485-488 (2003).
38. I. G. Gut, Y. Hefetz, I. E. Kochevar, and F. Hillenkamp, "Two-photon absorption cross sections of guanosine 5'-monophosphate and uridine 5'-monophosphate at 532 nm," J. Phys. Chem. **97**(19), 5171-5176 (1993).
39. C. E. Powell, J. P. Morrall, S. A. Ward, M. P. Cifuentes, E. G. A. Notaras, M. Samoc, and M. G. Humphrey, "Dispersion of the Third-Order Nonlinear Optical Properties of an Organometallic Dendrimer," J. Am. Chem. Soc. **126**(39), 12234-12235 (2004).
40. M. Samoc, A. Samoc, A. Miniewicz, P. P. Markowicz, P. N. Prasad, and J. G. Grote, "Polarization dependent nonlinear absorption and refraction: polarization modulated Z-scan and thermal lensing detected two-photon absorption," in preparation (2006).
41. Y. P. Svirko and N. I. Zheludev, *Polarization of Light in Nonlinear Optics* (John Wiley and Sons, Chichester, New York, Weinheim, Brisbane, Singapore, Toronto, 1998).
42. P. N. Prasad, *Introduction to biophotonics* (Wiley & Sons, Hoboken, New Jersey, 2003).
43. P. R. Monson and W. M. McClain, "Polarization dependence of the two-photon absorption of tumbling molecules with application to liquid 1-chloronaphthalene and benzene," J. Chem. Phys. **53**(1), 29-37 (1970).
44. I. Tinoco, Jr., "Two-photon circular dichroism," J. Chem. Phys. **62**(3), 1006-1009 (1975).
45. B. Jansik, A. Rizzo, and H. Agren, "Response theory calculations of two-photon circular dichroism," Chem. Phys. Lett. **414**, 461-467 (2005).
46. R. DeSalvo, M. Sheikh-bahae, A. A. Said, D. J. Hagan, and E. W. Van Stryland, "Z-scan measurements of the anisotropy of nonlinear refraction and absorption in crystals," Opt. Lett. **18**(3), 194-196 (1993).
47. A. N. Egorov, O. B. Mavritsky, A. N. Petrovsky, and K. V. Yakubovsky, "Nonlinear Optical Studies of C60, C70, and C60 Metal Derivatives under Picosecond Laser Excitation," Laser Physics **5**, 1006-1013 (1995).

48. S. M. Kennedy and F. E. Lytle, "p-Bis-(o-methylstyryl)benzene as a Power-Squared Sensor for Two-Photon Absorption Measurements between 537 and 694 nm," Anal. Chem. **58**, 2643-2647 (1986).
49. T. Xia, D. J. Hagan, M. Sheikbahae, and E. W. Vanstryland, "Eclipsing Z-Scan Measurement of Lambda/10^4 Wave-Front Distortion," Opt. Lett. **19**(5), 317-319 (1994).
50. J. A. Hagen, J. G. Grote, N. Ogata, J. S. Zetts, R. L. Nelson, D. E. Diggs, F. K. Hopkins, P. P. Yaney, L. R. Dalton, and S. J. Clarson, "DNA photonics," Proc. SPIE, **5351**, 77-86 (2004).
51. A. Samoc, M. Samoc, and M. Woodruff, "Photophysical processes involved in creation of dark spatial solitons in composite photonic media," Mol. Cryst. Liq. Cryst. Sci. Technol., Sect. A, 1058-1725X (1994).
52. L. De Boni, J. J. Rodrigues Jr, D. S. dos Santos Jr, C. H. T. P. Silva, D. T. Balogh, O. N. Oliveira Jr, S. C. Zilio, L. Misoguti, and C. R. Mendonca, "Two-photon absorption in azoaromatic compounds," Chem. Phys. Lett. **361**, 209-213 (2002).

APPENDIX

List of publications and conference proceedings incorporating results obtained under this research program

Journal papers:

1. A. Samoc, A. Miniewicz, M. Samoc, and J. G. Grote, "Refractive Index Anisotropy and Optical Dispersion in Films of Deoxyribonucleic Acid (DNA)," J.Appl.Polym.Sci. submitted (2006).
2. M. Samoc, A. Samoc, and J. G. Grote, "Complex nonlinear refractive index of DNA," Chem. Phys. Lett. submitted (2006).
3. M. Samoc, A. Samoc, A. Miniewicz, P. P. Markowicz, P. N. Prasad, and J. G. Grote, "Polarization dependent nonlinear absorption and refraction: polarization modulated Z-scan and thermal lensing detected two-photon absorption," in preparation (2006).

Conference presentations:

1. M. Samoc and A. Samoc, DNA photonics at the ANU: plans and thoughts. *International Workshop on DNA photonics, Hapuna Beach, Hawaii*, *27-31 March 2005*
2. M. Samoc, A. Samoc, A. Miniewicz and J. G. Grote, Femtosecond Z-scan studies of cubic nonlinear optical properties of salmon DNA. *Australian Conference on Optics Lasers and Spectroscopy, ACOLS, Rotorua, NZ, 5-9 Dec. 2005*
3. A. Samoc, M. Samoc, A. Miniewicz, and J.G. Grote. Linear and nonlinear refractive indices of deoxyribonucleic acid (DNA)*, ISOPL4 Conference, Dingle, Ireland, 27-30 June 2006*
4. M. Samoc, A. Samoc, A. Miniewicz, P.P. Markowicz and P.N. Prasad, Polarization dependent nonlinear absorption and refraction, *ISOPL4 Conference, Dingle, Ireland, 27-30 June 2006* (invited talk)
5. A. Samoc, M. Samoc, J. G. Grote, A. Miniewicz, B. Luther-Davies, Optical properties of deoxyribonucleic acid (DNA) polymer host, *SPIE Meeting "Optical Materials in Defence Systems Technology III", Stockholm 11-14 September 2006* (invited talk)